MPA Lectures - Alternatives Models of Dark Matter: Ultra Light fields

Elisa G. M. Ferreira

Max-Planck-Institut für Astrophysik, Karl-Schwarzschild-Str. 1, 85748 Garching, Germany

Contents

Acknowledgment

These notes have the goal of giving a very short review of the ultra-light dark matter candidates. This class of models is described in the literature with many different names and different constructions. To my knowledge there is no review that includes all of these models describing their differences and similarities. This is what I attempt in these notes: to give a very general and brief overview of the motivation for proposing this class of models, describe the physics of Bose Einstein condensation and superfluidity that is used to define them, and then try to classify the different ultra-light DM models present in the literature showing the different mechanisms they invoke to achieve condensation on galactic scales.

Since there is no unique general literature that I based this note on, but a series of articles referring to specific topics, then the main references used are cited in the corresponding sections. The only exception is Section 2 that is based mainly in the following reviews [1–3].

In the entire notes natural units are used.

1. Introduction and Motivation

There is an overwhelming amount of evidence from galactic to cosmological scales that support the need for a dark matter component. Even with this amount of evidence, the nature of the dark matter is still unknown. This is one of the oldest unsolved problems in cosmology and it can be traced back to the year of 1930's [4, 5]. It is also one of the better measured ones, since there are plenty of (indirect) evidence of its presence ranging from several scales. The first evidence for dark matter was found studying the rotation curves of galaxies. From pioneer studies [6] it was already evident that the amount of matter necessary to fit the flat observed rotaiton curve did not match the theoretical curve predicted, assuming Newtonian mechanics and taking into account only the visible matter present in those galaxies. Dark matter was proposed as an additional (non-luminous) matter to explain this discrepancy. Nowadays, the evidence for dark matter comes from precise measurements on very different scales. From sub-galactic and galactic scales, to clusters scales, going to up to the large cosmological scales. On cosmological scales, the observed anisotropies of the Cosmic Microwave Background (CMB) [8], together with measurement of the Type Ia Supernovae, measured the total energy density of matter with high precision. This together with the bounds on the abundance of the light chemical elements from the Big Bang Nucleosynthesis, which constraints the amount of baryonic matter in the universe, strongly shows the need for a clustering component of non-baryonic[1] origin, that does not interact (strongly) with photons, and that dominates the matter content of the universe, accounting for approximately 85%. The same non-luminous and clustering component, that is sufficiently cold, is necessary to explain the structures we see in our universe today, as it is evident in measurement of the large scale structure of our universe [7, 9].

With all this evidence coming from precise astrophysical and cosmological observations, cosmologists have converged to a phenomenological model to describe our universe, the ΛCDM model. The ΛCDM model is currently the concordance model of cosmology. This model accumulates a number of observational successes and exhibits an outstanding agreement with current cosmological observations [7], which is manifested in the parameters of this model being constrained at the level of 1%. This incredibly simple model is described by only 6 parameters and parametrizes a large amount of the universe's history. It describes a universe that is flat and seeded by nearly scale invariant perturbations, composed by baryons, which amount to approximately 5% of the energy density of the universe, a small radiation component, but in its majority is composed by two unknown components. The energy budget of the universe is dominated ($\sim 70\%$) by a component responsible for the current accelerated expansion of the universe called dark energy, and a clustering component, the dark matter, making up to $\sim 25\%$ of our universe. These large-scale observations give a coarse-grained description of these non-baryonic components in the hydrodynamical limit where dark matter is described as a (perfect) fluid with very small pressure ($w \sim 0$) and sound speed, $c_s \sim 0$, that does not interact with baryonic matter. Dark energy is parametrized by a cosmological constant, the simplest form of getting the late accelerated expansion of our universe.

So, the Cold Dark Matter (CDM) paradigm emerged from the large scale observations and describes the component responsible for the formation of the structures of our universe through gravitational clustering. This component must be massive, sufficiently cold, which means non-relativistic at the time of structure formation, and colisionless in order to explain the observational data in large linear scales. This coarse-grained description of a CDM is very successful in fitting the linear, large scales observations from the CMB, LSS, to clusters, and general properties of galaxies.

[1] We are going to see later that there are some "baryonic candidates for DM.

Within the CDM paradigm, many models for the nature of the DM were proposed. The possibility that dark matter could be a long lived particle, specially given by some expected candidates from fundamental particle physics, is very appealing. One class of models that became the preferred candidates for the DM particles are WIMPS, weakly interacting massive particles, which represent a new elementary particle that interacts with ordinary particles not only gravitationally but through the weak force. The strong motivation for this candidate is because if it is thermally produced in the early universe, the relic abundance of particles that have mass on the scale of masses of electroweak interaction, and coupling of order one, the abundance of WIMPS corresponds precisely to the abundance of DM in our universe. The possibility that WIMPS could also be detected by direct detection experiments is also an important motivation to search for this candidate. There is a great experimental effort to constraint the properties of WIMP DM with the parameter space being very constrained in the past few years. Given the complex phenomenology from the possible models of WIMP dark matter and their interaction with the SM particles, the translation of those bounds to the exclusion of WIMPS models is not straightforward. This scenario is currently being probed by direct, indirect detections and colliders.

We still have no conclusive evidence for electroweak or other non-gravitational interactions for dark matter, and all the knowledge we have about dark matter is only gravitational and the microphysics of the DM component is still unknown. So we need to find ways of exploring the microphysical properties of this component.

As the observations and simulations of the smaller non-linear scales and galactic scales improve, a number of challenges have emerged for this coarse grained description from ΛCDM. These discrepancies have been around for decades like the cusp/core problem, the missing satellite problem and the too big to fail problem. A particularly curious challenge is the regularity/diversity of rotation curves. One thing that is striking about galaxies is that they are extremely diverse, but at the same time they are incredibly regular. This is embodied in various empirical scaling relations. The most famous of which is the Baryonic Tully Fisher relation (BTFR), which tells us that the total baryon mass (including stars and gas) of the galaxy is related to the asymptotic rotation velocity in galaxies. The measured BTFR follows a scaling relation different than the predicted by the ΛCDM valid for a range of masses of 6 generations, with very small scattering. The significance of these discrepancies is disputed and addressing these challenges is an active field of research. Those challenges emerge in scales where baryonic physics is relevant and simulations including several baryonic effects have been perfected more and more pointing in the direction that baryons could explain some of these observations within ΛCDM.

As the physics of these baryonic processes is complex and there is no final consensus about the status of theses discrepancies, an alternative explanation for these discrepancies on small scales could be that DM is not the usual CDM, but a more complex component that has different dynamics on small scales. With that, the dynamics on small scales can offer a chance to probe the properties of DM in the hope to help find the microphysics of this component. The simplest modifications that can address some of the small scales discrepancies is warm dark matter (WDM) [11], where DM has a small mass leading to a thermal velocity dispersion, small enough so it does not spoil the large scale prediction of CDM. Even with a small velocity, DM free streams out of potential wells and is enough to suppress the formation of small scales structures addressing some of the small scale problems. Another popular model inspired by those discrepancies is the self interacting DM (SIDM) [13], where the DM models interact in a way to also suppress the formation of structures on small scales.

In the past few years, another class of alternative models has emerged offering a different mechanism to explain the dynamics on small scales. In this class of models, DM forms a Bose-Einstein condensate (BEC) or a superfluid on galactic scales. The idea is that the wave nature of DM on astrophysical scales modifies the dynamics on small scales, while maintaining the successes of CDM on large scales. For that, these models are composed by ultra-light bosonic fields that are produced non-thermally in the universe. An example of such non-thermal relic is the axion, and the connection axions with the phenomena of Bose-Einstein condensation on small scales attracted a lot of attention for these models. There are many ways that such a macroscopic quantum phenomena can be modelled in galaxies. For this reason there

are many different models in the literature that aim to address the small scale challenges using different realizations of this phenomena. The goal of this note is to describe these models in detail, explaining the different ways those achieve condensation in galactic scales, and showing their astrophysical and cosmological consequences.

Collecting all the requirement from the large scales observations, together with the discrepancies on small scales, the unknown nature of dark matter produced a enormous zoo of possible models of DM. We are focusing in the class of models of Ultralight DM. In these notes I will first describe the small scale challenges of the ΛCDM, as a motivation to show the discrepancies these alternative models of DM want to address. Next, I will introduce the basic concepts of those quantum phenomena of BEC and superfluids, so we can in the following section apply those concepts for the case of DM.

2. Small Scale Challenges of Cold Dark Matter

The ΛCDM model is considered the concordance model in cosmology since it has proven to be extremely successful in describing and predicting the cosmological observations at large scales. On small scales, the formation of structures is highly non-linear and the evolution of structures is studied using large numerical simulations. As those simulations and the observations of galaxies improved, a number of discrepancies between them started to emerge. Given the enormous success of the concordance model, these discrepancies attract a lot of interest of the community. They might represent that we need to better take into account the astrophysical processes that happen inside those regions, which indeed have a complex dynamics. Or this might indicate that the CDM model is not good to describe the physics on small scales and the coarse grained CDM paradigm needs to be revised. A even a more radical approach might say that we need to modify gravity on smaller scales.

In this section we present very concisely the theory of non-linear structures evolution. We show how the numerical predictions assuming the concordance model might be in conflict with the current observations of galaxies. These tensions are seen in the counts and density of low-mass objects, and in the scaling relations that show the tight regularity that galaxies present.

2.1. Dark Matter Halos and Substructures

A halo can be defined as virialized spherical mass concentrations of dark matter. They are formed by gravitational collapse of a non-linear overdense region that stopped expanding to collapse into a sphere in virial equilibrium[2]. The virialization of the halo happens through violent relaxation, where the DM particles scatter on small fluctuations of the gravitational field present in this distribution, taking a time t_{dyn}, the dynamical time, to fully cross the sphere. After this process is complete, at t_{coll}, the dark matter halo has a radius approximately 1/6 of the radius of the region it collapsed from, and average density [14]:

$$\langle\rho\rangle = (1+\delta_{vir})\,\bar{\rho}(t_{coll})\,, \tag{1}$$

where $\bar{\rho}$ is the mean density, and $(1+\delta_{vir}) \approx 178\,\Omega_m^{-0.6}$. Given this, the dark matter halo is defined as the spherical region where the density is approximately 200 the critical density of the universe at a given redshift, with mass given by:

$$M_{200} = \frac{4\pi}{3} R_{200}^3 200 \rho_{cr}\,, \tag{2}$$

where $\rho_{cr} = 3H^2(z)c/(8\pi G)$. The virial velocity is given by the circular velocity at the virial radius, $V_{200}^2 = GM_{200}/R_{200}$. With that, one can express the evolution of the mass and virial radius, with respect to V_{200}: $M_{200} = V_{200}^3/10\,GH(z)$ and $R_{200} = V_{200}/10H(z)$. We can see from these expressions that halos

[2]Virial equilibrium means that it obeys the virial theorem $E_{kin} = -2\,E_{pot}$ and conservation of energy. So we can describe the system by only R and M (or V).

that form early in the evolution of the universe are less massive, while late-forming halos are more massive and larger.

This definition is not unique and depends on the choice of the virial overdensity parameter Δ, which above was taken to be $\Delta = 200\rho_{cr}/\bar{\rho}$. More generally, (2) can be written as $M_{vir} = (4\pi/3)\, R_{vir}^3\, \Delta\, \bar{\rho}$. The values of Δ can vary in the literature, with some common definitions being $\Delta = 333$ at $z = 0$ for a fiducial cosmology given by [8], which asymptotes to $\Delta = 178$ at high-z [15]; or a fixed $\Delta = 200$ at all z, usually denoted by M_{200m}.

We identify the DM halos from numerical simulations and can extract from them the abundance of halos as a function of their mass for a given redshifts.

In the numerical simulations we can also analyze the individual halos, obtaining their radial mass profile. A surprising feature encountered in those simulations is that halos appear to have a universal density profile, averaged over spherical shells. Their functional form is characterized by the Navarro, Frenk and White profile [16]:

$$\rho(r) = \frac{\rho_s}{(r/r_s)\,(1 + r/r_s)^2} \rightarrow \begin{cases} 1/r\,, & \text{for } r \ll r_s \\ 1/r^3\,, & \text{for } r \gg r_s \end{cases} \tag{3}$$

where r_s is the radius where the slope of the profile changes and $\rho s = \rho(r_s)$. We can see that this profile diverges towards the center of the halo, presenting a cusp. The amplitude of the density profile can be written in terms of R_200, as we can see from (2):

$$\bar{\rho} = \frac{3}{4\pi R_{200}} \int_0^{R_{200}} 4\pi r^2 \rho(r) dr = 3\rho_s \int_0^1 \frac{x^2}{cx\,(1 + cx)^2}\,, \tag{4}$$

where $x = r/R_{200}$, and $c := R_{200}/r_s$ is the concentration index and describes the shape of the distribution. With that, the NFW profile can be determined completely by R_{200} (or M_{200} or any other halo radius definition), and the c. The shape of the concentration can be inferred from simulations, where $c \propto (M/M^*)^{-1/9}\,(1 + z)^{-1}$. We can see that as we saw above, early-forming halos have a smaller radius, and they are denser than the larger ones, given the higher concentration. The NFW profile can be generalized for a three parameters profile that fits better the DM profile of halos for all range of masses [17–19].

2.2. Discrepancies in Comparison with Observations

In this section we will show how some of theoretical predictions from simulations of the small scales considering the ΛCDM model compare with respect to astrophysical observations. However, this comparison is not straightforward, since we indirectly probe the dark matter inferring it from the visible matter that traces the gravitational potential on galaxies and clusters. There are a few approaches to connect the informations of galaxies and the dark matter halo like forward modelling, abundance matching and kinetic measurements, and each of those methods has its difficulties and limitations. The result of this comparison is a series of discrepancies that challenges the results of the simulations, and in some cases limitations in observations. I will present some of these challenges in this section. Some of those challenges might have complementary origin and solution, and are indeed connected, as we will discuss bellow.

To aid in this discussion, I give a small summary of the conventions used throughout this paper when comparing to observations. For most of the challenges we will be discussing dwarf galaxies, which implies galaxies with masses smaller than $10^9\, M_\odot$. Regarding their mass, they can be further divided into Bright dwarfs ($M \sim 10^{7-9} M_\odot$), Classical dwarfs ($M \sim 10^{5-7} M_\odot$), and ultra-faint dwarfs ($M \sim 10^{2-5} M_\odot$). Regarding their characteristics, the dwarfs can be divided into spheroidals which are usually satellites, that have no gas and no star formation, and irregulars, that contain gas and star formation.

2.2.1. Cusp-Core Problem

As we saw above, the expected density profile from colisionless simulations is the NFW profile which is cuspy towards the central region of the halo. Given the complex dynamics of baryonic matter in

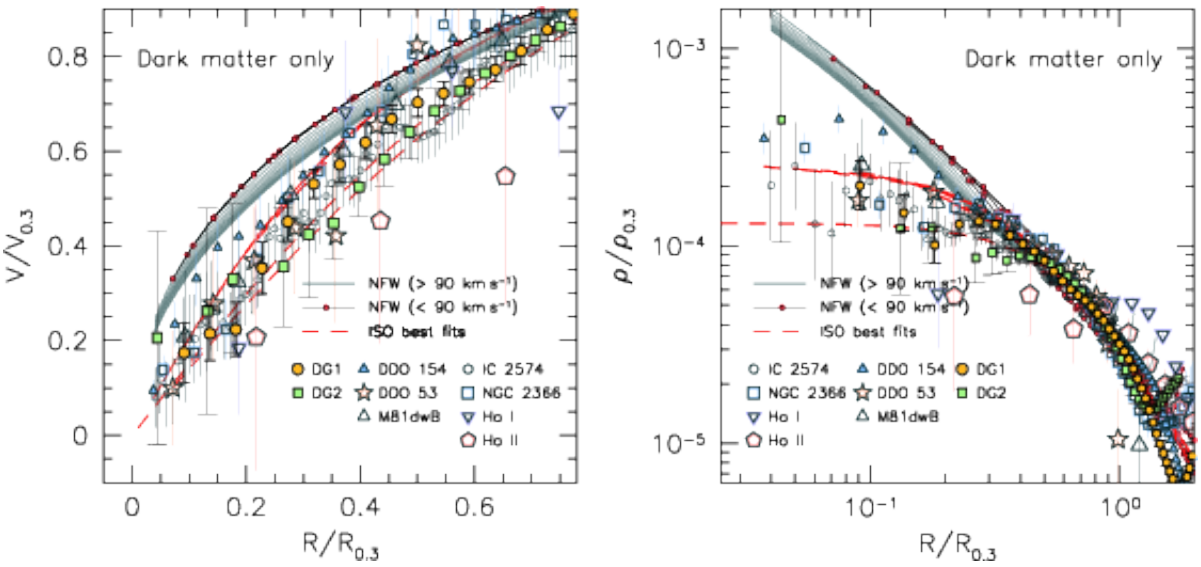

Figure 1: In this plot we show the results from the THINGS survey [34]. *Left panel:* Comparison of the RCs from (a) 7 dwarf galaxies from THINGS; (b) two simulated galaxies DG1 and DG2,, to the NFW (solid lines), and pseudo-isothermal (ISO) profiles (red dashed line). The NFW RCs with V200 in the range 10–90 km/s are highlighted by small red dots. The rotation velocity V is scaled to $V_{0.3}$, namely the value of V at $R_{0.3}$, representing the distance at which $dlogV = 0.3$. *Right panel*:same conventions as the left, but for the density profiles.

some galaxies, good laboratories to probe the halo structure are low-surface brightness (LSB) galaxies and late-time dwarfs. Those systems are dominated by DM throughout their halo up until the central regions. Measuring the rotation curves of dwarf galaxies, [20, 21] found that those measurement preferred cored isothermal profiles. Many other measurements of the rotation curves of those systems [22–33] have confirmed this discrepancy, showing that a constant density core with a profile with a slope $\gamma = 0 - 5$ (considering the profile at small radius given by $\rho \sim 1/r^{\gamma}$). The smallest values for this slope from dissipationless simulations are too large to in comparison to the ones obtained by observations.

The recent measurement of nearby dwarf galaxies from the survey THINGS (HI Near Galaxy Survey) [34] and LITTLE THINGS [35] confirmed this discrepancy. Measuring the rotation curves from 7 and 26 nearby dwarfs, they found that the inner slope is much smaller than the NFW one -1, with $\gamma = 0.29 \pm 0.07$ for the LITTLE THINGS survey, as we can see in Figure 1.

The situation is more complex for high surface brightness objects given its complex inner density structure; or for galaxies with large mass, like spiral galaxies, where at small radii is dominated by baryonic matter; and for dwarf spheroidals that show a strong dependence of the bias in the modelling of the system. Even in the case of dwarf galaxies, it was pointed out that some systems present cuspy profiles, while others cored ones, presenting an unexpected diversity in the rotation curves [36]. Since different results were obtained by different techniques for the same system, this shows that determining the inner slope of galaxies is a hard task.

The origin for these discrepancies can come from the fact that the simulations take into account only DM, while the properties of galaxies are also influenced by the presence of baryons. The newest hydrodynamical simulations obtained by many independent groups, have shown that baryonic feedback can in fact soften the inner cusps in the profile and generate core-like profiles like the ones observed for dwarf galaxies.The main effects are supernova feedback flattening and dynamical friction from baryonic clumps (for a more detailed list of these and other baryonic processes see [2]). These simulations show a threshold mass of $M_{vir} \sim 10^{10} M_{\odot}$ bellow which the simulation predict profiles that are cusped [37–42].

However, not all simulations agree with this result. Additionally, modelling those baryonic feedback effects is challenging, and introduce many new parameters and uncertainties in modelling assumptions. Finally, not all baryonic processes that might influence the formation and dynamics of galaxies were

included in the simulations, and that might reveal to be important for the result. It is clear that the inclusion of baryonic effects are hinting in the right direction, but until consensus is achieved, alternative need to be considered. As mentioned before, a modification of the properties of DM might in a simple way account for that, as we will show for the case of Bose Einstein condensate DM. An early solution to the cusp-core problem, and that explains the rotation curves with exquisite precision is a modification of the dynamics of gravity on small scales, the MOdified Newtonian Dynamics (MOND). This is also a solution for the regularity versus diversity challenge, and I will present its main points and shortcomings in the end of this section.

2.2.2. Missing satellites and too big to fail

Structure formation is hierarchical in nature and it is expected that the DM halos are also populated by small subhalos. This is confirmed in ΛCDM simulations of Milky-way sized halos, which show that the subhalo mass function diverges toward low masses, limited only by the numerical limit. Those simulations then predict several hundreds of subhalos with $v_{max} \sim 10-30$km/s, that are large enough to host a galaxy ($M_{peak} \leq 10^7 M_\odot$). On the other side, until 2005 only 12 MW classical satellites were known, with 15 more confirmed ultra-faint satellite galaxies until 2014, with the data from Sloan Digital Sky Survey(SDSS) [43]. To date, with inclusion of Dark Energy Survey (DES) data, a few more ultra-faint candidates were discovered, with the known count of satellites of more than 50. However, the number of MW galaxies is still much smaller than the predicted from simulation. This discrepancy not only appears in the MW, but also in the Local Group. This is known as the missing satellites problem.

DES and future observations are expected to discover more of those ultra-faint galaxies, which can alleviate this discrepancy, but there is still debate if will solve the problem. Another possibility is that low-mass subhalos are there, but we just cannot see them, since they have very low baryonic content. One can expect that for low mass subhalos, galaxy formation is suppressed since the photoionizing background heats the gas, reducing its cooling rate and inhibiting gas accretion for $M_{vir} \sim 10^9 M_\odot$ [44–48]. Star formation is also suppressed since supernova-driven winds could strip the gas out of these halos [49]. Other mechanisms can also suppress the baryon content in the low-mass galaxies, see [2]. So, the visible subhalos are only a set of the entire distribution of halos that contains the non-visible faint end. It was shown recently in hydrodynamical simulations [50–52] that apparently this mechanisms can solve the discrepancy between the predicted to observed number of satellite galaxies, solving the missing satellite problem. However, there are still some missing low-mass satellites.

This mechanism that solves the missing satellite problem leads to another challenge: the too big to fail. When we say that the visible subhalos of the MW are only a set representing the most massive subhalos in the total distribution of subhalos, to have agreement with ΛCDM simulation these visible MW subhalos need to correspond to the most massive subhalos predicted by the simulation. But, the most massive subhalos predicted by those simulations have central masses ($V_{max} > 30$km/s) that are too large to host the observed satellite galaxies [53, 54], and the ones that have central mass like the expected by the MW (with $12 < V_{max} < 25$km/s) are not most massive ones. So, the puzzle is why should the most massive subhalos, where the gravitational potential is the strongest and the striping gas mechanisms cited above are not important, be too big to fail at forming galaxies.

This problem also appears in the galaxies in the Local Group and Local Volume [56, 57].

Like for the other problems, it was proposed that some astrophysics processes driven by baryons could be important on those scales and solve the too big to fail. However, these solutions seem to only work for the MW. This is an intense topic of debate and, to my knowledge, no consensus has been reached. As these notes were being written, there has been claims that the the too big to fail problem has been solved [58].

As for the cusp core problem, different DM physics could solve those problems, by having a mechanism that suppresses the formations of small scales subhalos, and that reduces the central densities of massive subhalos (or modifies the dynamics of the central regions). We are going to show how the models with Bose Einstein condensation addresses some of those problems.

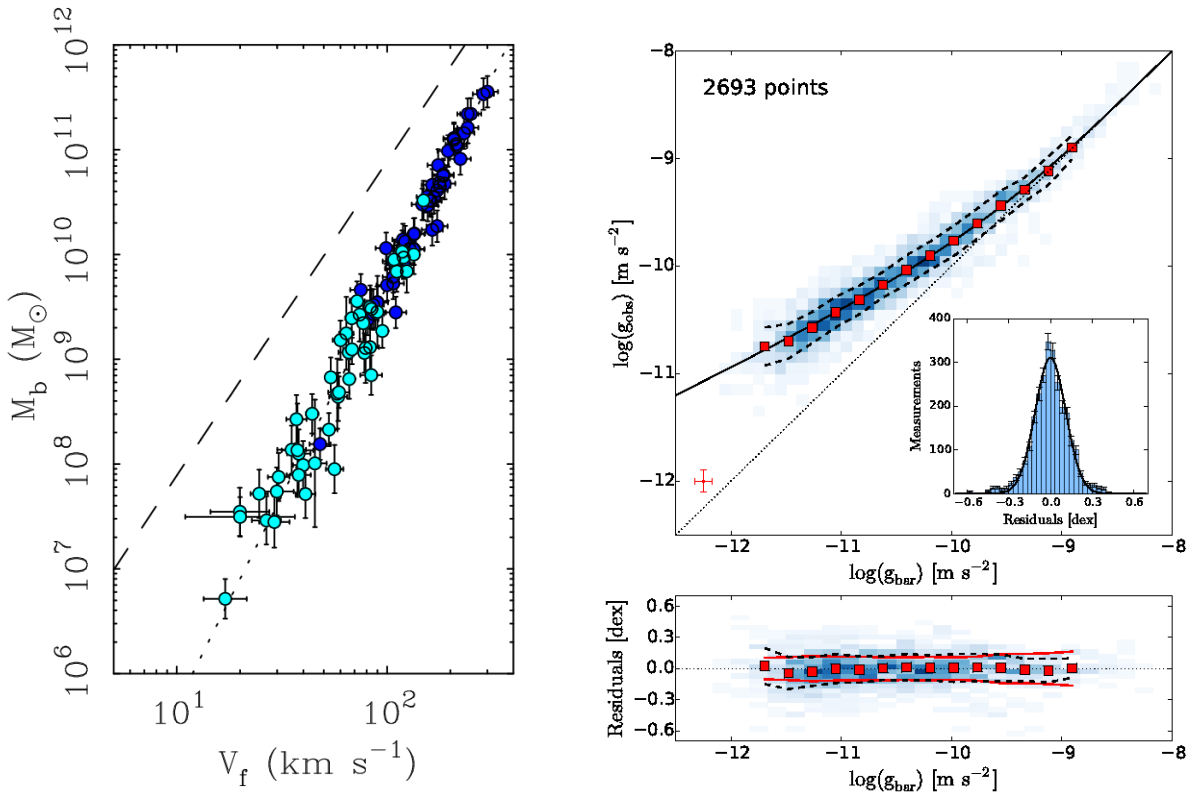

Figure 2: *Left panel:*The figure shows Baryonic Tully Fisher Relation (BTFR) from [3], which shows the relation between the baryonic mass (M_b) and the asymptotic circular velocity for galaxies for high resolution galaxies with observed extended rotation curves. The dark blue points represent star dominated galaxies, and the light blue points gas-dominated ones. The dashed line has slope 3, as expected by the ΛCDM; while the dotted line has slope 4. *Right panel:* Plot of the Radial Acceleration Relation from [62], for 153 SPARC galaxies. The lower panel shows the residuals, and the red uncertainty bar shows the mean uncertainty on individual points. The solid line represent the fit to the data while the dotted line is the unit line. The insert is a histogram of the residuals.

2.2.3. Diversity vs. Regularity: Scaling Relations

One thing that is striking about galaxies is that they are extremely diverse, but at the same time they are incredibly regular. This regularity is embodied in various empirical scaling relations, that are shown to hold very tightly for a diverse range of galaxies. These relations relate the dynamical and baryonic properties of galaxies, and hold even for DM dominated systems, and they are one of the most tantalizing aspects of galaxy phenomenology, representing the most pressing challenge to ΛCDM on small scales.

The most famous of those relations is the Baryonic Tully Fisher relation (BTFR) [60, 61], which relates the total baryon mass (including stars and gas) of the galaxy to the asymptotic circular velocity in galaxies, V_f (this is the velocity measured at the flat portion of rotation curves):

$$V_f^4 = a_0 G_N M_b \,, \tag{5}$$

where a_0 is the critical acceleration, a scale that appear in observations. Its value can be obtained from the data and given by $a_0 \sim 1.2 \times 10^{-8}$cm/s. The BTFR is an extension of the Tully Fisher relation, which related the luminosity, instead of the mass, to the circular velocity. It extends the validity of the scaling relation of many decades in mass. This empirical scaling relation is show to hold for large ranges of masses, 6 generations, with a very small scatter, compatible to the size of the error bars. The left panel of Figure 2 presents the BTFR. As we can see, the slope of the BTFR is different that the predicted by ΛCDM, $V_f^3 \propto M_b$, shown in the dashed line.

However, there is a even more important challenge: the mass discrepancy acceleration relation (MDAR). The MDAR is a remarkably tight correlation between the dynamical gravitational acceleration inferred

from rotation curves ($g_{obs} = V^2/r$) and the gravitational acceleration due to baryons only (g_{bas}), as inferred from the distribution of stars and gas [62, 63], as we can see in the right panes of Figure 2. This relation shows us that in regions of high acceleration, where $g_{obs} > a_0$, where baryons dominate, you have $g_{obs} \sim g_{bar}$. For low accelerations, in the central regions where it is expected to be DM dominated, this relation deviates from the unit line. In plain DM parlance, the MDAR implies that by looking only at the baryon mass distribution, one can infer the DM density profile at every radius in the galaxy, even in galaxies where baryons are everywhere subdominant. At large distances in the disk, the MDAR implies the BTFR.

These empirical relations, coming directly from observations, show a surprising feature that in galaxies the dynamics is dictated by the baryon content, even when DM dominates. Even more unexpected these relations are very tight, showing very little spread, even if they came from very diverse types of galaxies. As pointed out in [1], in these correlation what dictates the dynamics is the baryon mass, which is the sum of gas and stars, and not only the stellar mass, which is the one that is expected to correlate more with the total feed energy. Recently it was shown by many groups that these relations can be explained within the ΛCDM paradigm [73–77] using the latest hydrodynamical simulations like EAGLE [83, 84], APOSTLE [85], Illustris [82], ZOMG [78–80], and NIHAO [81]. Those simulations include several baryonic effects (like star formation, stellar evolution, metal enrichment, gas cooling/heating, galactic outflows and BH feedback, among others) to their ΛCDM simulations[3]. Those new large volume and very accurate simulations, like Illustris, and EAGLE, have also been able to reproduce the features of the rotation curves of galaxies within ΛCDM. So, it is very encouraging the huge amount of progress on the simulation side.

Some questions still remain, though. In these references, indeed the BTFR and the MDAR trend can be reproduced in those simulations. However, as it is pointed out by most of the authors, the scatter obtained in the scaling relations is larger than the expected from data (some authors claim that this spread is correlated with the errors in the stellar feedback). A question remains then if this is a matter of improving the feedback models and/or resolution of the simulation, or if given the stochastic nature of the feedback effects will ever be able to give such tight correlations. Another point is that is important to be answered is about the importance of these baryonic feedbacks, since some of those authors claim that the results are not very sensitive to the feedback model, which is intriguing. Those simulations also still don't go all the way until dwarf galaxies[4], which are DM dominated and where most of the tension is. In summary, most progress has been done on the simulation side with results that are very encouraging to explain the formation and dynamics of galaxies. But the simulation are still not enough and still do not fully reproduce the observations.

2.3. MOND empirical law

As we cited above, the small scales challenges of the CDM can be solved by adopting one of the following approaches: including baryonic effects or by modifying the DM physics. However, another proposal for solving some of the puzzles of galactic evolution known as MOdified Newtonian Dynamics proposes something more radical: a universe without DM that has a modified force law for small accelerations.

Milgrom, in 1983, motivated by the scaling relations and rotation curves of galaxies, made a remarkable observation about the mass discrepancy in galaxies. He observed that the mass discrepancy can be determined by the observed baryonic matter, and it can be described in the simple empirical law:

$$a = \begin{cases} a_N\,, & \text{for } a_N \gg a_0\,, \\ \sqrt{a_0\, a_N}\,, & \text{for } a_N \ll a_0\,, \end{cases} \tag{6}$$

[3] In these notes I will not enter in the details of such baryonic effects that are taken into account in those simulations. This is a field of its own, very rich and fast developing, and discussing those effects is not the scope of these notes.

[4] To my knowledge. But as I said, it is a fast moving field.

where $a_N = G_N M_b(r)/r^2$ is the Newtonian acceleration. The scale a_0 appears naturally from observations, like we saw in the previous subsection, and its value can be fitted by the data giving $a_0 \sim 1.2 \times 10^{-8}$cm/s^5. This scale separates the regimes where the centripetal acceleration experienced by a particle at large accelerations is given purely in terms of the Newtonian (baryonic) acceleration, and at small acceleration, where the acceleration is given by the geometric mean of both accelerations.

The MOND works beautifully fitting the rotations curves of galaxies. Specially in HSB, which are dominated by baryons in the inner regions, this empirical law captures the features of the rotation curve that should have a raise, from the inner region which is described by the Newtonian baryonic acceleration, followed by a Kleperian fallout to the flat part of the rotation curve. LSB galaxies (which were predicted by Milgrom), are DM dominated, or in the language of MOND, have low accelerations, given their low stellar surface density, from the center to the outer regions. So their rotation curves is characterized by a slow raise of the rotation curve, approaching the flat part, which is reproduced by MOND. It is also remarkably successful in explaining the empirical scaling relations (for a review see [3, 69–71]).

On top of the empirical relation above, that is proven to work very well to explain the galactic regime, Milgrom made further assumptions to construct his theory, which I will call full MOND theory. The theory assumes that there is no DM in the universe and that MOND gives a modification of gravity. In order to try to get the empirical law (6) as a modified gravity theory, Berkenstein and Milgrom [72] described an effective theory for MOND. This can be accomplished by having a scalar field coupled to gravity with effective Lagrangian:

$$\mathcal{L}_{MOND} = -\frac{2M_{pl}^2}{3a_0}\left[(\partial\phi)^2\right]^{3/2} + \frac{\phi}{M_{pl}}\rho_b\,, \tag{7}$$

which represents a scalar field with a non-canonical kinetic term that is conformally coupled to matter. This Lagrangian, for static and spherically symmetric source, results in a modified Poisson equation:

$$\vec{\nabla}\cdot\left(\frac{|\vec{\nabla}\phi|}{a_0}\vec{\nabla}\phi\right) = 4\pi G_N\rho\,, \qquad \phi' = \sqrt{a_0\frac{G_N M(r)}{r^2}} = \sqrt{a_0 a_N}\,. \tag{8}$$

So, this theory describes that on top of the Newtonian force, there is a scalar field mediated force, which is given by the MONDian acceleration. This is a simplified version of their theory, since in their theory they have a way of making an interpolation between the different regimes. This theory also has a fractional power kinetic term, that may give raise to problems of superluminal propagation.

Nowadays, with the huge successes of ΛCDM on large scales, specially the CMB anisotropies and lensing observations, any theory that does not have DM is not compelling. MOND also cannot explain galaxy cluster, since it does not predict an isothermal profile. Many attempts were made to extend MOND, by including DM, or extending it to relativistic regimes, beyond others (see reviews cited above). However, the empirical relation (6) is incredibly successful. That alone, without the assumptions of full MOND (no DM and modified gravity), even in the context of ΛCDM, is a powerful statements about how DM is distributed in galaxies: in regions where baryons dominate, the theory behaves like Newtonian theory, and in regions where the DM dominates, the DM mass is uniquely determined by the baryonic distribution, $G_N M(r)/r = \sqrt{G_N M_b(r) a_0}$.

Given the shortcomings of the full MOND, but the great successes of the empirical law, instead of trying to obtain this theory from a fundamental Lorentz invariant theory, having a theory of DM where the dynamics of MOND emerges at galactic scales it is a way of leveraging on the successes of the empirical theory and of the large scales. This is done in the theory of DM Superlfuid that will be presented in Section 4.

[5] A funny numerical coincidence if that the measured scale a_0 is related to the Hubble parameter today, $a_0 \sim (1/6)H_0$. Does this indicate something?

Since the nature of DM is still not known, and since the newest simulations and observations still did not give definitive evidence that those discrepancies can all be explained by baryonic effects, it is interesting and valid to investigate modifications of the DM paradigm. Different models of dark matter can affect the formation of structures in distinct ways, both in the linear and in the non-linear regimes. So the small scales offer an opportunity to probe the microphyics of DM, beyond the hydrodynamical large scale CDM paradigm. The non-linear regime can be specially changed by modifications of this paradigm, with galaxies being a sensitive probe of DM. This could help finding new properties of DM, that can be predicted and measured, that could help elucidate the nature of DM.

We are going to study in this review models where the small scale behavior is characterized by the formation of a Bose Einstein condensate in galactic scales. In those models, DM forms a coherent state in the central core of galaxies, modifying the physics in these scales. We have many different ways in which this can be implemented by having pure Bose Einstein condensates or superfluids with different types of interactions, and each of those can yield different modifications of the small scales and also different predictions. Those models, tough, rely on the quantum mechanical effect of Bose Einstein condensation and superfluidity, applied to a context very different than where they were discovery in the realm of condensed matter physics. In the next section we present a small review of the physics of Bose Einstein condensate and superfluid as an introduction to the section where we describe dark matter as having those properties.

3. Bose-Einstein Condensation and Superfluidity

In this section we present a short review of Bose-Einstein Condensation and Superfluidity. We aim to give an introduction to the basic theory, properties and the methods used to describe those systems, so they can be applied for the case of DM in the next section. The different methods to describe those systems and their limit of validity are very important to be able to understand the construction and validity of the models presented next.

Bose Einstein condensation is one of the most fascinating phenomena of quantum mechanics. Since it was theorized in the year of 1920's, its experimental realization opened the door for many advances in the physics of many-body systems, and even to the application of this phenomena in other fields of like in cosmology. In a simple way, Bose Einstein condensation happens when at very low temperatures a large fraction of the bosons of a system occupy the lowest quantum state, the ground state of a configuration. This macroscopic occupancy of the lowest energy state is a consequence of bosons following the Bose statistics which allows them to be at the same quantum state, at thermal equilibrium, different than fermions that suffer from the Pauli exclusion principle. This transition to the ground state bellow a low critical temperature is seen, in thermodynamics and statistical mechanics, as a phase transition that happens in the system resulting purely from the quantum statistics of bosons. It is an inherently quantum mechanical phenomena since in this phase transition the de Broglie wavelength of these bosons superpose and form a coherent wavelength describing this new state of many-particles (or atoms).

A few years after the discovery of Bose Einstein condensates (BEC), another intriguing macroscopic quantum mechanical phenomena was discovered: superfluidity. In 1937, Pyotr Kapitsa [86] and independently John Allen and Donald Misener [87], conducting experiments with helium-4 realized that after cooling down this liquid to a certain temperature, the fluid starts flowing without friction, even climbing the walls of the container where it was stored. Fluids that exhibit this behaviour, characterized by a zero viscosity, are called superfluids. Landau provided a phenomenological description of this effect which rendered him the Nobel prize in 1962. It was proposed by Fritz London, after the development of laser cooling techniques for atomic gases, that the properties of He^4 superfluid are related to BEC. This was not obvious given that the (textbook) description of BEC as an ideal non-interacting Bose gas, while He^4 is an interacting fluid. This was confirmed years latter in ultracold atomic gases that almost the entire fluid at low temperatures is condensed and exhibits superfluidity.

A weakly interacting Bose gas was then proposed as a modification of the non-interacting Bose gas model, in order to explain the superfluidity in liquid helium, where superfluidity is described as being achieved through interactions in a BEC. In this way, superfluids are modelled by a Bose Einstein condensate that has self-interaction. The BEC represents the ground state of the system, while the superfluidity is a property of the excitations of this condensate. Notice that BEC can happen even in the absence of self-interaction, as cited above, since it is a statistical property of a gas of bosons in low temperature, but this system does not exhibit superfluidity.

In this section we will describe first the non-interacting BEC gas, or pure BEC, and show the properties and conditions for condensation. Following that, we show the definition of superfluidity as defined in Landau's theory of superfluid. Next, we show that condensation in systems that have a self interaction, and consequently exhibit superfluidity. This quantum mechanical system is described by the non-linear Schroedinger equation, called the Gross-Pitaevskii equation. This equation describes the evolution of the wave function of the condensate, in the mean field approximation. From that we can derive the hydrodynamical description of this system, given by the Mandelung equation. We then show the field theory description of the BEC, which brings advantages and makes clear the study of many features in BECs and superfluids.

Not linked to this note, but an important fact. Nowadays, it is known that superfluidity is not necessarily linked to condensation. Recent investigations seems to point that there are states where you can have superfluidity for the majority or all the particles in the system, while only a small fraction is condensed. This happens for example for liquid helium bellow a certain temperature.

3.1. Pure BEC: Ideal Bose Gas

We start our discussion with the non-interacting Bose gas. The properties of this system are a consequence purely from the quantum statistic of indistinguishable bosons. We will see that in the grand canonical ensemble we can write the Bose distribution function in which we can see the conditions for Bose Einstein condensation.

To describe a gas where many particles are present and they can access many states, we need an ensemble description to be able to describe the probabilities of occupation of the states. A grand canonical ensemble (GCE) described by the chemical potential (μ) and the temperature (T) holds for a system in contact with a large reservoir, in a way that there is exchange of energy and particles with the reservoir, conserving those constants. The grand canonical ensemble probability to realize a configuration with $N^{'}$ particles in a state k with energy E_k is [89]:

$$P_{N'}(E_k) = e^{\frac{1}{k_B T}\left(\mu N' - E_k\right)}\,, \tag{9}$$

The chemical potential $\mu = (\partial E/\partial N)_{S,V}$ is the energy required to add one particle to the the isolated system, it is defined to be negative (so no unphysical negative occupation occurs), and it is determined by N, the total number of particles, and T. If we start from a Hamiltonian to describe the gas, the independent particle Hamiltonian $\hat{H} = \sum i\hat{H}_i^{(1)}$, the grand canonical function partition function can be worked out exactly and we get the same description.

With this probability, we can calculate the GCE partition function $Z(T,\mu) = \sum_{N'}^{\infty}\sum_k P_{N'}(E_k)$. The GC potential can be readly calculated from this: $\Omega = -k_B T \ln Z = E - TS - \mu N$. With that, we are able to calculate the total number of particles:

$$N = -\frac{\partial \Omega}{\partial T} = \sum_i \frac{1}{\exp\left[\frac{1}{k_B T}(\epsilon_i - \mu)\right] - 1} = \sum_i n_i\,, \tag{10}$$

where $N^{'} = \sum i n_i$, and $E_k = \sum i\epsilon_i n_i$, given that n_i is the microscopic occupation number and ϵ_i the energy density.

We can separate the total number of particles into two contributions:

$$N = N_0 + N_T \,, \tag{11}$$

where $N_0 = 1/\left[\exp\left[\frac{1}{k_B T}(\epsilon_i - \mu)\right] - 1\right]$ and $N_T = \sum_{i\neq 0} n_i$ is the number of particles out of the condensate and also called the thermal component of the gas. We can replace the sum for an integral and, from the partition function:

$$N_T = \frac{V}{\lambda_T}\int_0^\infty d\epsilon \frac{\epsilon^{1/2}}{e^{\frac{1}{k_B T}(\epsilon-\mu)}} \,, \tag{12}$$

where $\lambda_T = \sqrt{2\pi\hbar^2/(k_B T)}$. When $\mu \to \epsilon_0$, the occupation number N_0 of the lowest energy state grows larger and larger. While that N_T grows but is bound to a maximum N_c (associated to a critical temperature T_c), the number at maximum chemical potential $\mu = 0$. As the number of particles in the ground state grows, it becomes macroscopically occupied. This phenomenon is called Bose Einstein condensation. The temperature T_c defines the temperature bellow which BEC happens.

After defined the criteria for BEC, we can evaluate the number of particles in the condensate. One can also show that, for $T < T_c$, N_T integral can be evaluated and that actually $N_T = N\,(T/T_c)^{3/2}$. In this way, from (11) we can write the number of particles in the condensate as:

$$N_0/N = n_0 = 1 - \left(\frac{T}{T_c}\right)^{3/2} \,. \tag{13}$$

From that expression we can see that the occupation becomes macroscopic towards small temperatures. This condition for the critical temperature T_c for when the condensation happens can be translated to $n\lambda_{dB}^3 \gg 1$, where $\lambda_{dB} = \sqrt{2\pi\hbar/(mk_B T)}$ is the thermal de Broglie wavelength that gives the coherence length of the gas. So, when this occurs, the de Broglie wavelength of the particles overlap and the system is described by a macroscopic wave-function.

In summary, Bose Einstein condensation can happen for ideal gases. The condition for condensation is that the occupation number of the ground state is so large that becomes macroscopic, this happens when $T < T_c$ there is formation of BEC; and for $T > T_c$ there is no condensation. This can be translated in a *condition for condensation*: if $n\lambda_{dB}^3 \gg 1$, there is the formation of a BEC; and if $n\lambda_{dB}^3 \ll 1$, there is not. For such large occupation, the quantum corrections are suppressed, and the BEC can be written as a good approximation in terms of classical theory. We are going to see that for an interacting theory, the a classical field theory with spontaneous symmetry breaking is a good description for a BEC system.

3.2. Landau's superfluid model and criteria for superfluidity

Landau constructed his general theory to explain the results of the superfluidity in Helium, which was observed to flow in capillaries. However, the theory is quite general and gives general conditions for superfluidity.This theory aims to explain why in superfluids charge is transported without friction. The main ingredient for that is a BEC which carries charge and can flow without losing energy. Excitations on top of this condensate can lead to dissipation. We need to set the condition for this excitations to allow superfluidity.

Consider a superfluid moving through a capilar with velocity v_s. In the rest frame of the capillary, the energy of the elementary excitations is given by [89]:

$$E = E_{kin} + \epsilon_p + \mathbf{p}\cdot\mathbf{v}_s \,, \tag{14}$$

where E_{kin} is the kinetic energy of the fluid, and $\epsilon_p > 0$ and $\mathbf{p}$ are the energy of the excitation and momentum in the frame of the fluid, and translated to the frame of the capillary. Dissipation happen when $\epsilon_p + \mathbf{p}\cdot\mathbf{v}_s < 0$. This can only be negative if its minimum, when $\epsilon_p + pv_s\cos(\theta)$ when $\theta = n\pi$ for n integers, is smaller than zero: $\epsilon_p - pv_s < 0$. With that we can determine the critical velocity:

$$v_c = \min_p \frac{\epsilon_p}{p} \,. \tag{15}$$

So, for $v < v_c$, the system transports charge without dissipation and the coherence of the BEC is maintained. The complete criteria for superfluidity is the existence of a condensate, otherwise there is nothing to transport the charge without friction; v_c cannot be zero (like it is the case for the non-interacting Bose gas, where $v_c = 0$); and the above criteria, $v < v_c$.

As we are going to see in the next section in the case of the weakly interacting BEC that because of the spontaneous breaking of the U(1) symmetry, a Goldstone mode appears. This mode is gapless $\epsilon_{p=0} = 0$. Even for that mode, the critical velocity is not zero, so there is some cost for producing the gapless excitation. We will also see later that, this gas obeys Landau's criteria and the critical velocity is the fluid sound speed. With that, Landau's criteria for transport without dissipation in a weakly superfluid is given by:

$$v_s < v_c = c_s \,. \tag{16}$$

And given that v_c is nonzero, a that we have a condensate (by construction) in this system, if the above criteria is met, we can say that there is superfluidity. This results is only valid for $T = 0$.

Landau also developed the theory for a superfluid at finite temperature, the *two fluid model*. At finite temperatures the fluid has two components: the **superfluid** component that flows without friction, and a **normal fluid** which describes the excitations. In this theory then there are two sounds, for each degree of freedom. In the case of weakly interacting Bose gas, the first sound is c_s associated with the oscillation in density, and the second sound is $c_s/\sqrt{3}$ that corresponds speed of propagation of a temperature oscillation.

3.3. Interacting BEC

Superfluidity is an effective dynamics presented by the collective excitations of a BEC at low temperatures. This was showed above described by Landau's phenomenological theory, where the role of the condensate is not clear, and just effectively describe the flow of a frictionless fluid. A microscopic description of this system consists of an interacting many-body system of boson that form a condensate at low temperatures. The dynamics of the condensate at zero temperature with interaction or in a trapping potential is usually given by the Gross-Pitaevskii theory, where we describe the evolution of the wave function of the condensate through a non-linear Schroedinger equation, the Gross-Pitaevskii equation. This theory describes effectively a mean-field approximation for the interparticle interactions and it gives the main quantitative properties of the system.

The N-body Hamiltonian describing N interacting bosons can be written, in the second-quantized formalism:

$$\hat{H} = \sum_{ij} H^{sp}_{ij} \hat{a}^\dagger_i \hat{a}_j + \frac{1}{2} \sum_{ijkm} \langle ij|\hat{V}|km\rangle \hat{a}^\dagger_i \hat{a}^\dagger_j \hat{a}_k \hat{a}_m \,, \tag{17}$$

where $\langle ij|\hat{V}|km\rangle$ denotes the matrix element for the interaction, and $H^{sp}_{ij} = \int d^3\mathbf{r} \tilde{\Phi}^*_i(\mathbf{r}) \hat{H}^{sp} \tilde{\Phi}_j(\mathbf{r})$, where $\tilde{\Phi}_j$ is the states wavefunctions . The single particle Hamiltonian is given by $H^{sp} = (1/2m)\nabla^2) + V_{trap}$, where V_{trap} is the trapping potential, that could be, as we will see in the next sections, the gravitational potential. The creation and annihilation operators, $\hat{a}^\dagger$ and $\hat{a}$, create and annihilate a particle from the state $\tilde{\Phi}_j$. They obey the Bose commutation relations: $[\hat{a}_i, \hat{a}^\dagger_j] = \delta_{ij}$ and $[\hat{a}_i, \hat{a}^\rfloor_j = 0$.

The wavefunction $\tilde{\Phi}_0(\mathbf{r})$ describes the condensate, while the remaining functions form a complete set of functions orthogonal to the condensate. We can rewrite this Hamiltonian in terms of a continuum spectrum of single particle position eigenstates:

$$\hat{\Psi}^\dagger = \sum_i \hat{a}^\dagger_i \tilde{\Phi}^*_i(\mathbf{r} \,, \qquad \hat{\Psi} = \sum_i \hat{a}_i \tilde{\Phi}_i(\mathbf{r} \,. \tag{18}$$

The operator $\hat{\Psi}$ is the Bose field operator, which obeys the same commutation relation than $\hat{a}$. The Hamiltonian in terms of these operators reads:

$$\hat{H} = \int d\mathbf{r} \hat{\Psi}^\dagger(\mathbf{r}) \hat{H}^{sp} \hat{\Psi}(\mathbf{r}) + \frac{1}{2} \int d\mathbf{r} d\mathbf{r}' \hat{\Psi}^\dagger(\mathbf{r}) \hat{\Psi}^\dagger(\mathbf{r}') V(\mathbf{r} - \mathbf{r}') \hat{\Psi}(\mathbf{r}) \hat{\Psi}(\mathbf{r}') \,. \tag{19}$$

This Lagrangian is invariant under U(1) symmetry. This Hamiltonian although can be used to obtain the properties of the system, it is very hard to be calculated given the large value of particles. To simplify, we use *mean-field* approximation. In this approximation, the wavefunction can be written, in the Heisenberg picture as:

$$\hat{\Psi}(\mathbf{r},t) = \psi(\mathbf{r},t) + \delta\hat{\Psi}(\mathbf{r},t)\,, \tag{20}$$

where $\psi(\mathbf{r},t) \equiv \langle\hat{\Psi}(\mathbf{r},t)\rangle$ is classical field called the wavefunction of the condensate and has the meaning of an order parameter[6]. The density of the condensate is fixed by: $n_0 = |\psi(\mathbf{r},t)|^2$. Like we described for Landau's theory, $\delta\hat{\Psi}(\mathbf{r},t)$ is a small perturbation of the system and describes depletion of the condensate.

From the above Hamiltonian, and given this mean-field approximation, we can write the Hamilton equation for ψ:

$$i\partial_t\psi(\mathbf{r},t) = \left(-\frac{\nabla^2}{2m} + V_{trap}(\mathbf{r}) + U_0|\psi(\mathbf{r},t)|^2\right)\psi(\mathbf{r},t)\,. \tag{21}$$

This is the Gross-Pitaevskii equation, that describes the evolution of the order parameter. Writing the condensate wavefunction as:

$$\psi(\mathbf{r},t) = \phi(\mathbf{r})e^{-i\mu t}\,, \tag{22}$$

where ϕ is real field and normalized to the total number of particles, $\int d\mathbf{r}\phi^2 = N_0 = N$. The Gross-Pitaevskii equation can be written as:

$$\left(-\frac{\nabla^2}{2m} + V_{trap}(\mathbf{r}) + U_0\phi^2(\mathbf{r})\right)\phi(\mathbf{r}) = \mu\phi(\mathbf{r})\,. \tag{23}$$

This is a non-linear Schroedinger equation. The non-linear term is proportional to the number density $n = \phi^2$, and comes from the mean-field approximation. This condensate eigenvalue is given by the chemical potential μ.

Some comments are in order. When defining ψ as the condensate wavefunction, this quantity that is actually a mean-field value of the wavefunction, the degree of freedom that defines the condensate. This description of averaging selecting the condensate is consistent with the theory of critical phenomena, like phase transitions. This Bose system can be seen as a system with spontaneous breaking of a symmetry of the description. In our case the U(1) symmetry which is the symmetry of the Hamiltonian. This is analogous to the the spontaneous symmetry braking in a ferromagnet. The difference is that, since we have a Bose system, the idea of spontaneous symmetry breaking to the thermodynamical limit of a finite size Bose gas defines the number of particles of the system, and this is only consistent with the picture of having a condensate that can change the number of particles in the ground state, if the number of particles is conserved.

With that, the interacting condensate system above can be understood as a particle conserving system of bosons with U(1) symmetry, described by the classical field ψ, the wavefunction of the condensate, where the formation of a Bose Einstein condensate is a phase transition, coming from a spontaneous breaking of the symmetry (that can be seen as spontaneous coherence). This description of the condensate makes us see a parallel with the formalism used in *field theory*.

Field theory. The methods from field theory are very appropriate to describe the system above. So, in a field theory formalism, a weakly interacting Bose system can be thought as a system carrying a conserved U(1) charge (the number of particles) in a state that has finite density charge and that spontaneouly breks the U(1) symmetry. The spontaneous breaking is caused by the finite charge. So, a system that

[6]In a theory where phase transition happens, which is the case here, the order parameter determines the order of the system: when the symmetry is broken and the system is "ordered" is non-vanishing; and it vanishes in the restaured phase, called "disordored".

describes this is given by the 2-body interacting Lagrangian for the complex scalar field[7].

$$\mathcal{L} = |\partial_\mu \Psi|^2 - m^2|\Psi|^2 - \lambda|\Psi|^4\,, \tag{25}$$

where $\lambda > 0$ for stability. This is exactly the Lagrangian a scalar field theory with 2-body interaction.This Lagrangian is invariant under U(1), so $\Psi \to \Psi e^{-i\alpha}$. Here *alpha* is a constant, which mean the U(1) is a global symmetry. To describe the condensate, like we did previously, we expand the field $\Psi = \phi + \delta\Psi$, where ϕ is the condensate and $\delta\Psi$ are the fluctuations.

For the condensate, the symmetry broken regime, we can write the complex field as

$$\phi(X) = \frac{\rho(X)}{\sqrt{2}} e^{i\Theta(X)}\,, \tag{26}$$

where the phase $X = (\mathbf{x}, x_0)$. Putting this back into the Lagrangian we can see that Lagragian has a homogeneous part and an interaction part: $\mathcal{L} = \mathcal{L}^{(0)} + \text{fluctuations}$, where:

$$\mathcal{L}^{(0)} = \frac{1}{2}(\partial_\mu \rho)^2 + \frac{\rho^2}{2}\left[(\partial_\mu \Theta)^2 - m^2\right] - \frac{\lambda}{4}\rho^4\,. \tag{27}$$

The conserved current is given by $j^\mu = \rho^2 \partial^\mu \Theta$. We can integrate out ρ in the limit ρ is constant, we have that:

$$\rho = 0\,, \qquad \rho^2 = \frac{(\partial_\mu \Theta \partial^\mu \Theta) - m^2}{\lambda}\,. \tag{28}$$

and from the conserved current $\partial_t j_0 = \rho^2 \partial_t \Theta = \text{const.} \Rightarrow \partial_t \Theta = \mu$, is the chemical potential. For $\mu^2 < m^2$ is the symmetry restoring phase; and $\rho^2 = (1/\lambda)(\mu^2 - m^2)$ is the symmetry breaking phase. The relativistic Bose Einstein condensation happens then, when $\mu^2 > m^2$ [8].

So, the symmetry is broken by the ground state $\Theta = \mu t$. Or, as seen in the Lagrangian in the footnote, by the term with the chemical potential.

We also need to calculate for the perturbations $\delta\Psi$. We can also expand it as$\delta\Psi(X) = \delta\Psi_0(X) e^{-i\theta(X)}$, where θ is the Goldstone boson associated with the breaking of the U(1) symmetry, the phonon excitations. By calculating second order Lagrangian for the perturbations, it is easy to obtain the dispersion relation for the Goldstone boson, which is linear in the momentum. One can also determine the sound speed of the fluid, which is important for Landau's condition for superfluidity. At low energies, given that the phonon is massless, this is the only excited mode of the theory, and the massive ones can be integrated out. So, a superfluid is described by a theory of the evolution of the phonon.

Recovering the other approaches. Starting from our field theory for the weakly interacting bosons we can recover the other approaches to describe our superfluid system: the Gross-Pitaevskii equation and the hydrodynamical equations. Lets start with (25). We are interesting in taking the non-relativistic limit of the Lagrangian. For this we rewrite the fields as:

$$\Psi(X) = \frac{1}{2m}\psi(X) e^{-imt}\,, \tag{29}$$

and take the non-relativistic limit. With that, the Lagrangian can be written as:

$$\mathcal{L} = \frac{i}{2}\left(\dot{\psi}\psi^* - \psi\dot{\psi^*}\right) - \frac{1}{2m}|\nabla\psi|^2 - \frac{\lambda}{16m^2}(\psi^*\psi)^2\,. \tag{30}$$

[7] An alternative way of writing this Lagrangian that leave explicitly the spontaneous breaking of the symmetry by the finite charge:

$$\mathcal{L} = |(\partial_\mu - i\mu)\Psi|^2 - m^2|\Psi|^2 - \lambda|\Psi|^4\,. \tag{24}$$

This is equivalent to the usual way we introduce the chemical potential in the Hamiltonian: $\mathcal{H} - \mu\mathcal{N}$, where $\mathcal{N} = j^0$ is the conserved charge.

[8] The non-relativistic chemical potential must always be smaller than zero. The relativistic chemical potential is $\mu_{rel} = \mu_{NR} + m$.

The equation of motion for ϕ is:

$$i\dot{\psi} = \left(-\frac{1}{2m}\nabla^2 + \frac{\lambda}{8m^2}|\psi|^2\right)\psi\,, \tag{31}$$

which is exactly the Gross-Piatevskii equation like shown above, in the absence of a trapping potential.

From that, we can also derive the Mandelung hydrodynamical equations. If we make the following substitution:

$$\psi \equiv \sqrt{\rho/m}e^{i\theta}\,, \qquad \mathbf{v} \equiv \frac{1}{m}\nabla\theta\,. \tag{32}$$

The vorticity of the superfluid is zero and the momentum density has a non-zero curl. Plugging this in the equations of motion, we have that:

$$\dot{\rho} + \nabla\cdot(\rho\,\mathbf{v}) = 0\,, \tag{33}$$

$$\dot{v} + (\mathbf{v}\cdot\nabla)\mathrm{v} = \frac{\nabla\mathbf{p}}{\rho}\,. \tag{34}$$

These are the conitnuity and Euler equations modified for our system. The last term in the Euler equation is the pressure that arises due to the self-interaction of the field. This set of equations is the Mandelung equations, the hydrodynamical equations that describe the evolution of the superfluid.

In this section we showed how to describe a weakly interacting BEC, that exhibits superfluidity, in the mean-field approximation using the field theory approach, the Gross-Pitaevskii approach and the hydrodynamical one. We can see that they are equivalent in some regimes. The choice of which description to use depends on the observables you want to verify from the theory.

About the validity of the description. The theory presented above is only valid for zero temperatures and in the mean-field approximation. The fields can be treated as classical if $n\lambda_{dB} \gg 1$, like stated in the pure BEC section, the limit where quantum corrections are not important.

In the case of finite temperatures, the above theory needs to be modified, and the system should be described by a two fluid finite field theory model. Attempts to do that exist in the literature. Also, if one wants to go beyond mean field approximation, there are many descriptions that allow that (see [89] for some examples). In the cases we are going to study, we will extend a bit the validity of the zero temperature description, as a first approximation, since in galaxies the temperature is obviously not zero. However, since the occupation number will be very high in our problem, the classical description is safe.

3.3.1. Effective field description of a superfluid

We described in the previous section the construction of a EFT for the weakly interacting BEC that can be used to describe superfluids. This description is based on London's idea, that has its roots in the superfluid/superconductor hydrodynamics, that the BEC can be described by a theory with spontaneous symmetry breaking where the symmetries of the theory are described by the Nambu-Goldstone boson. The EFT generated by this procedure is shown to be able to describe the behavior of the superfluid, matching many observations, in the low energy and momentum regimes. It is expected that simple extensions to this Lagrangian can yield the Schrodinger equation that is able to describe different phenomena, like for example superconductivity. However, this does not work properly [90]. When this procedure is done, the Nambu-Goldstone does not behave as they should and it does not obey the hydrodynamical identity,

$$T_{0i} = mj_i\,, \tag{35}$$

which states that all the momentum and current is carried by a single species with mass m. This relation should be respected in the hydrodynamical limit of superfluids.

And it is not only for superconductivity. The interacting BEC description above is also not able to describe other phenomena in condensed matter physics like the unitary Fermi gas, which is a gas of fermions that interact through a strong 2-body coupling. The ground state of the unitary Fermi gas is a

superfluid. This theory was measured experimentally, and some features are described in some regimes theoretically using Thomas-Fermi theory or superfluid hydrodynamics. But this is limited and it does not describe the physics at wavelength slightly larger than the healing length. To add corrections at this limit is not possible since in this strong coupling theory we cannot build a reliable perturbation theory. So, we need to find another description of superfluidity and other phenomena like superconductors that is more general in order to encompass a larger class of models, like the ones cited here, where the weakly interacting BEC description does not work. For that we need to exploit all the symmetries of these systems and build an EFT that can more generally describe these phenomena in the long-wavelength limit [91].

Inheriting the knowledge of a superfluid from previous sections, at low energies, the only dynamical degree of freedom that describes a superfluid is the phase of the condensate, the phonon. So, in this non-relativistic regime, we need to construct the EFT of this phase, θ from $\psi = |\psi|e^{-}i\theta$.The superfluid is described by a theory where the symmetry is spontaneously broken by the ground state:

$$\theta = \mu t - \phi \,, \tag{36}$$

where ϕ are the phonon excitations. This theory has shift-symmetry $\theta \to \theta + c$ inherited from the U(1) symmetry of the complex scalar field. With that, if we want to construct the EFT for the phonon, from the rules of EFT we have to write all the terms that are compatible with the symmetries of the problem. One of the symmetries is shift symmetry. In order for the Lagrangian to be invariant under this symmetry, only terms that are acted by a derivative can appear in the theory:

$$\mathcal{L} = \mathcal{L}\left(\dot{\theta}, \partial_i \theta\right) \,. \tag{37}$$

This may contain terms with any power of the derivative of the field.

However, this theory has more symmetries. In a generic space-time and adding a gauge field, which is a natural extension of the simple scalar field model, we require that this Lagrangian is invariant with respect to three-dimensional general coordinate transformations and gauge invariance. The most general Lagrangian $\mathcal{L} = \mathcal{L}\left(D_t\theta, g^{ij} D_i D_j \theta\right)$ that is invariant under these symmetries, shift symmetry, gauge invariance and general coordinate invariance, is given by:

$$\mathcal{L} = P\left(X\right) \,, \qquad X = D_t\theta - \frac{g_{ij}}{2m} D_i\theta D_j\theta \,, \tag{38}$$

where $D_t\theta = \dot{\theta} + A_0$ and $D_i\theta = \partial\theta - A_i$. In flat space, $g_{ij} = \delta_{ij}$, the general coordinate invariance corresponds to a Galilean symmetry[9]. In the absence of gauge fields $A_0 = A_i = 0$, the Lagrangian that describes this system is given by:

$$\mathcal{L} = P\left(\dot{\theta} - \frac{(\partial_i\theta)^2}{2m}\right) \,. \tag{39}$$

This is a Lagrangian that has a non-canonical kinetic term and it obeys (35). One limit of this Lagrangian is the quadratic Lagrangian for the weakly interacting BEC. This action obeys naturally (35) and it is also invariant under the general coordinate transformations[10].

If one wants to add a trapping potential V_{ext}, like for example if the gas is under the influence of a gravitational potential, this corresponds to making $A_0 = Vext$. With that, the Lagrangian is given by (38), with $X = \dot{\theta} - \frac{(\partial_i\theta)^2}{2m} - V_{ext}$. In the case of the gravitation potential this is given by $X = \dot{\theta} - \frac{(\partial_i\theta)^2}{2m} - m\Phi$, where Φ is the gravitational potential.

[9] As it can be seen in [91], Galilean symmetry is not enough to constrain the NLO terms and one needs to consider the full general coordinate invariance.

[10] To describe a relativistic superfluid one has to impose Lorentz symmetry, which will give an effective Lagrangian, $\mathcal{L} = \mathcal{L}(T)$ where $T = -(1/2)g^{\mu\nu}\Theta_\mu\Theta_\nu$, and Θ is the relativistic phase coming from a relativistic complex field.

This Lagrangian density is, at zero temperature, the pressure as a function of the chemical potential $P = P(\mu)$, and it is related to the particle number density by:

$$n = P^{'}(X)\,, \tag{40}$$

where $'$ is the derivative with respect to A_0. The ground state $\theta = \mu t$ leads to $X = \mu$, and by the above relation $n(\mu)$ is the equilibrium number density at chemical potential μ. So, $P(\mu)$ is the thermodynamical pressure, defined up to a constant.

Given the Lagrangian (39) with $\theta = \mu t + \phi$ we can write the Lagrangian as:

$$L = P(\mu) - n\dot{\phi} + \frac{1}{2}\frac{\partial n}{\partial \mu}\dot{\phi}^2 - \frac{n}{2m}(\partial_i \phi)^2\,. \tag{41}$$

We can see from that the phonon speed of sound:

$$c_s = \sqrt{\frac{n}{m}\frac{\partial \mu}{\partial n}} = \sqrt{\frac{\partial P}{\partial \rho}}\,, \tag{42}$$

where $\rho = mn$ is the mass density.

With that Lagrangian we are able to describe the theory as the other approaches we used to describe the BEC and superfluid theories.

Superfluid hydrodynamics. From this formalism we can also describe the superfluid hydrodynamics. From (39) we can derive the continuity equation:

$$\dot{n} + \frac{1}{m}\partial_i\left(n\partial_i\phi\right) = 0\,. \tag{43}$$

We can identify the superfluid velocity with the gradient of ϕ, $\mathbf{v}_s = -\nabla\theta/m = \nabla\phi/m$, we can derive the second equation of superfluid hydrodynamics:

$$\dot{\phi} = -\mu(n) - \frac{m v_s^2}{2}\,. \tag{44}$$

Effective Hamiltonian. With that general Lagrangian we can also write the effective Hamiltonian. The conjugate momentum to the θ variable is: $\pi_\theta = \partial L/\partial\dot{\theta} = P^{'}(X) = n$. The only non-zero commutator is $[n(t,\mathbf{x}), \theta(t,\mathbf{x})] = -i\delta(\mathbf{x}-\mathbf{y})$. With that the Hamiltonian is:

$$H = n\dot{\theta} - P(X) = n\frac{(\partial_i\theta)^2}{2m} + \left(nX - P(X)\right)\,, \tag{45}$$

where $(nX - P(X))$ is the Legendre transform of $P(X)$ and give the energy with respect to n, $\epsilon(n)$. We can rewrite it as $H = \rho v_s/2 + \epsilon(n)$ which represents the kinetic energy of the superfluid flow and an internal energy not associated to the macroscopic flow.

In this section we were able to describe a general theory for superfluids as (38), that can be used in a larger number of cases: superfluids with different equation of state, strongly interacting superfluids, supercondutivity, unitary Fermi gas, among others. These superfluid models described with this approach can reproduce in the leading order the results from hydrodynamics of superfluids. However, this framework also allows us to go beyond leading order in this momentum expansion, the next-to-leading order (NLO) Lagrangian. This can be done in this framework at arbitrarily order, only requiring that the NLO Lagrangian respects the symmetry of the system, and at the cost of introducing new free parameters.

We are going to see that this general approach to describe superfluids is very useful to describe the superfluid in the DM superfluid model.

4. Ultra-Light DM

Ultra light field DM denotes a class of models where DM is composed by a light field that forms a Bose Einstein condensate or superfluid on galaxy scales. The wave nature is manifest on astrophysical scales, modifying the dynamics of DM on galactic scales. For this reason, it is an alternative way of addressing some of the small scale challenges of ΛCDM, while behaving as standard CDM on large scales. The idea of having DM condensation on small scales is not new and has been around for around 30 years [92, 93]. These models receive a lot of attention given their rich phenomenology on galactic scales while maintaining the successes of ΛCDM on large scales, and also because of their possible connection with axions, which are a strong candidate for DM. Axions can form a BEC given that they are non-relativistic, conserve number and are produced at high occupancy. Although this connection is very attractive, these models are much more general and the light DM particles do not need to be axions, only need to be very light particles that can condense into a BEC on small scales.

These models receives many names in literature and invoke condensation in similar but distinct ways that have important implications for the observables of the models. As far as I see, we can classify these models basically in three categories[11] (although not a very strict classification, since some models use simplification and might end up in the other category). Sometimes the names of these models are used interchangeably, but one needs to be careful about the distinctions in those models where condensation (and the consequent phenomena of this) are reached from different methods.

The first category is called *BEC DM* (or repulsive DM, scalar field DM, fluid dark matter, among others) [96–109]. In these models, the BEC has a 2-body self-interaction, which is responsible for superfluidity. So, it is the case of the interacting BEC presented above that exhibits superfluidity. The condensate has a long range coherence in the case of repulsive interaction. The 2-body case is characterized by having an equation of state (EoS), in the mean-field approximation, $P \sim n^2$, where n is the number density.

The second category is composed by models where there is no self interaction between the particles, and the particles are trapped only by the gravitational potential. Condensation occurs due to gravitational interactions, and stability is achieved at certain scales through quantum pressure. This class of model can be called *ultra-light DM* and it is highly studied in the literature. One of its main realization is the *fuzzy dark matter* model [113, 114], where the DM is given by a light particle with $m \sim 10^{-22}$eV. This model is also called wave DM, ψDM, among other names [92, 93, 110–112]. This model can be seen as a case of the interacting model above where the interaction is an attractive one given by gravity. In a model perspective this is true, but the mechanism that leads to the stability of the condensate is different than in the interacting case, where boson-boson interaction controls it, but given by the uncertainty principle. Given the absence of self interaction, and given that the gravitational interaction is very weak, as pointed out above, the low energy excitations are not phonon and superfluidity is not achieved.

In the case of the QCD axion, this was studied both in the contexts of BEC DM and ultra-light DM [115–117]. The validity of this description as a DM model was disputed in [118], where long-range coherence in the condensate can only be achieved in the presence of a repulsive interaction. We will describe this in details in the next subsection.

The third category is called *DM Superfluid* [120–124]. This model is also a model of an interacting BEC, and it is described as a strong self interacting theory of light boson that condenses into a BEC and exhibits superfluidity. This theory was proposed with the goal of on small scales, reproducing MOND, presenting a natural framework for the emergence of this theory. Different than in the case of BEC DM, so we can reproduce MOND on small scales it requires that the mean-field EoS is given by $P \sim n^3$. Given this EoS, this could be though as coming from an effective field theory, like the usual interacting BEC,

[11] This is a personal view, that overlaps with the one from the authors of [94]. But this is not how it is presented in all the literature like [95], which gives a extensive review of the current models. This classification is good because it elucidates the physics responsible for the condensation, and stability. These different mechanisms have consequences for the phenomenology of the models.

but with a 3-body interaction. As we will see bellow, this description does not work to give the proper Lagrangian of MOND.

Table 1: Classes of models that exhibit BEC or superfluidity on galaxes scales, dicriminated by the type of self interaction that the model has and their mean-field equation of state (EoS).

Model	Interaction	EoS
BEC DM	2-body	$P \sim n^2$
Superfluid DM	"3-body"	$P \sim n^3$
Ultra lighDM (*fuzzy DM*)	$\lambda = 0$ (Grav. interaction)	"Quantum pressure"

In summary, although all these models use the idea of Bose condensate DM in galaxies, given their different modelling, they present important differences. In ultra-light DM, the galactic dynamics is given by the condensate density profile, and given the large de Broglie wavelength from those particle, small scale structures are suppressed. In this case, phonons play no role. For the BEC DM and Superfluid DM, phonons are key and their dynamics control the galactic behavior. The difference in these models is that in the BEC DM the EoS is $P \sim n^2$, while for the DM Superfluid the EoS is $P \sim n^3$, which changes the condensate density profile and, more importantly, changes the sound speed of the phonon. The sound speed is an important criteria for being in a supefluid state or not, as shown in Landau's theory. So, this different sound speed affects where the DM is superfluid or not, and has important consequences for the validity of this theory on systems like the Bullet cluster. This will be discussed in more details in the next sections.

This list of models is not at all complete and it only aims to show the diversity of models in the literature. In [95] one can find a more complete list of references. Another review on some of those models is [119].

After this small review on the classification of the ultra-light scalar field models, in this section I will present them in detail, showing their properties and evolution on galactic scales, and showing how they address the small scale challenges. If we could describe the DM superfluid perfectly as a BEC with 3-body, we could describe all the three models using the formalism described in Section 3.3, just changing the the interaction term to a 2-body interaction for BEC DM (which give $P \propto n^2$), a 3-body interaction for the DM superfluid (which gives $P \propto n^3$), and no interaction, but a trapping gravitational interaction for Ultra-light DM. However, the DM superfluid model cannot be directly described by an interacting BEC with a 3-body interaction, since this will not give the wanted MOND behavior (more details of that are shown bellow). To describe the DM superfluid mode, we use the EFT developed in Section 3.3.1. For this reason, I will describe separately the two first models, and the DM superfluid. So, in this section I will first present a general description that can accommodate the first two models, the BEC DM and ultra-light DM, and then I will speciallize in the *fuzzy DM*. After that I will present the DM superfluid model.

4.1. Condensation in BEC DM and Ultra-light DM

In this section we will describe the general features of the BEC DM and Ultra-light DM models. We will describe them using the field-theory formalism for a interacting or trapped BEC done in Section 3.3.

We want to describe a class of the models cited above where a light scalar field is the DM component. This can be described as a very light scalar field ϕ, with a self-interaction that is minimally coupled to gravity given by the action:

$$S = \int d^4x\sqrt{-g}\left[\frac{1}{2}g^{\mu\nu}\partial_\mu\phi\partial_\nu\phi - \frac{1}{2}m^2\phi^2 - \frac{\lambda}{4!}\phi^4\right], \tag{46}$$

where $g_{\mu\nu}$ is the metric. If we wanted to specialize in the QCD axion, the potential in the Lagrangian above could be thought of coming from the QCD axion potential $V(\phi) = \Lambda^4(1-\cos(\phi/f_a))$ for small field

values ($\phi \ll f_a$), where $m = \Lambda^2/f_a$ are of order $\mathcal{O}(10^{-5})$eV, and $\lambda = -\Lambda^4/f_a^4 < 0$. In our case, this is a generic light scalar field.

Since the particles we are considering a very light, the Compton wavelength m^{-1} is much smaller than the particle horizon at matter domination, when we are interested in DM being responsible for the formation of structures and the behavior in galaxies. In this limit, we can use Newtonian approximation and the non-relativistic dynamics for the field. To consider the non-relativistic limit, we re-write the field as:

$$\phi = \frac{1}{\sqrt{2m}}\left(\psi e^{-imt} + \psi^* e^{imt}\right) . \tag{47}$$

Taking the non-relativistic limit ($c \to \infty$ if we recover the c's), we have can write the non-relativistic action as:

$$S = \int d^4x a^3 \left[\frac{i}{2}\left(\psi\partial_t\psi^* - \psi^*\partial_t\psi\right) - \frac{|\vec{\nabla}\psi|^2}{2m} - \frac{\lambda}{16m^2}|\psi|^4\right] , \tag{48}$$

where we are using a Friedmann Robertson Walker (FRW) metric given by:

$$ds^2 = (1+2\Phi)\,dt^2 - a^2(t)\,(1-2\Phi)\,d\mathbf{r}^2 . \tag{49}$$

This Lagrangian gives the following equation of motion:

$$i\dot{\psi} = -\frac{3}{2}iH\psi - \frac{1}{2ma^2}\nabla^2\psi + \frac{\lambda}{8m^2a^2}|\psi^2|\psi - m\Phi\psi . \tag{50}$$

If we consider time scales smaller than the expansion, we can ignore expansion and write the equation of our system as:

$$i\dot{\psi} = -\frac{1}{2m}\nabla^2\psi + \frac{\lambda}{8m^2}|\psi^2|\psi - m\Phi\psi , \tag{51}$$

which is a non-linear Schrodinger equation. The gravitational potential term can be re-written in the form $-Gm^2\psi\int d^3x'|\psi(\mathbf{x}')|^2/|\mathbf{x}-\mathbf{x}'|$. This non-linear equation is the Gross-Pitaesvkii equation cited above. We can use this equation to analyse the properties of this system, analytically and numerically.

We can also rewrite the field theory above as a fluid, or better, a superfluid that follow hydrodynamical equations, in this long wavelength limit. For that, if we identify (using the theory in the presence of expansion again):

$$\psi \equiv \sqrt{\frac{\rho}{m}}e^{i\theta} , \qquad \mathbf{v} \equiv \frac{1}{a\,m}\nabla\theta = \frac{1}{2im\,a}\left(\frac{1}{\psi}\nabla\psi - \frac{1}{\psi^*}\nabla\psi^*\right) . \tag{52}$$

The vorticity of the superfluid is zero and the momentum density has non-zero curl. The comoving equations of motion for ψ are:

$$\dot{\rho} + 3H\rho + \frac{1}{a}\nabla\cdot(\rho\mathbf{v}) = 0 , \tag{53}$$

$$\dot{\mathbf{v}} + H\mathbf{v} + \frac{1}{a}(\mathbf{v}\cdot\nabla)\,\mathbf{v} = -\frac{1}{a}\nabla\Phi + \frac{\nabla\mathbf{p}}{\rho} + \frac{1}{2a^3m^2}\nabla\left(\frac{\nabla^2\sqrt{\rho}}{\sqrt{\rho}}\right) . \tag{54}$$

where the first is the continuity equation and the second the Euler equation. These set of equations are the Mandelung equations, generalized for an expanding universe. The second term in the r.h.s. of equation (54) comes from the self-interaction term and p is pressure from the interactions. The last term in the equation for the velocity, if we had the factor of $\hbar$, would have $\hbar^2$ in front. This term represents the quantum pressure and resists compression. This is present even in the absence of interaction and it is going to be important for the effects and formation of the condensate for the fuzzy DM model. This form of the equations is useful for numerical simulations that can reveal some properties of the DM scalar field.

Conditions for condensation

The theory developed above of a self-interacting scalar field in a FRW universe is analogous to the theory for the weakly interacting BEC, so from our knowledge from last section, we know this will describe a BEC with superfluidity in the interacting case. From our knowledge of the ideal gas, we expect the free scalar field to thermalize and form a BEC. The condition for thermalization is that the occupancy number is very high, macroscopic, at $T < T_c$. This condition is then given by: $\bar{n} = n\lambda_{dB} \gg 1$. So, what are the conditions for this to happen in galaxies? Making a back of envelope calculation, $n = n_{gal}$ is the number density of the axion-like particles in our galaxy and λ_{dB} is the de Broglie wavelength given by:

$$n_{gal} = \frac{\rho_{gal}}{m}\,, \qquad \lambda_{dB} = \frac{2\pi}{mv}\,, \tag{55}$$

where ρ_{gal} is the density of particle in our galaxy, and v is the velocity of the dark matter halo. This gives a bound to the mass:

$$m < 4.7\text{eV}\left(\frac{\rho_{gal}}{10^9\text{eV/cm}^3}\right)\left(\frac{10^{-3}}{v}\right)^{3/4}\,. \tag{56}$$

For typical values of the galaxies like the Milky way, the density is of order $\rho_{gal} \sim 10^9\text{eV/cm}^3$ and velocity $v \sim 10^{-3}$, then the mass in order to have condensation must be smaller than 4.7eV. For masses of order $m \sim 10^{-22}$eV, the de Broglie wavelength is of order ~ 1.92kpc for the values above (with occupation number $\bar{n} \sim 10^{97}$). This value is of order (but smaller) than the size of a Milky Way-like galaxy (~ 30kpc). So, for such small masses, the influence of this collective behavior is manifest on galactic scales. For the QCD axion, with mass around $m_{axion} \sim 10^{-5}$eV, the occupation number is high, $\bar{n} \sim 10^{26}$ so condensation will happen, but the de Brogglie wavelength is of order $\sim 10^4$cm, which is much smaller than galaxies. So we need to investigate in more detail what astrophysical influence such a small condensate would have.

For an ideal gas, the equilibrium is obtained with all the particles in the ground state of the theory, which is the state with zero or very small k. From a field theory perspective, this is seen as the field evolving slowly with a very long-range correlation. This calculation is done using a $T = 0$ ideal gas general condition and we need to check the influence of the interaction and of a trapping potential, like the gravitational potential, have in the size of the coherent phase to see what scales are influenced by the BEC of these models. This is what we investigate next. We investigate now the stability around the condensate which shows us the coherence size of the condensate, and then show the ground state solution possible. We want to calculate this for the cases of BEC DM and for the Ultra-light DM, so we are going to separate into the self-interacting case and the free in a gravitation potential case.

BEC-DM: self-interactions

Evolution around the condensate and stability. Ignoring gravity, we want to investigate the effect of the self interaction in the model. The Schrodinger equation that describes this is:

$$i\dot{\psi} = -\frac{1}{2m}\nabla^2\psi + \frac{\lambda}{8m^2}|\psi^2\psi\,. \tag{57}$$

We decompose the field into a homogeneous, which represents the condensate, plus a perturbation part: $\psi(\mathbf{x}, t) = \psi_c(t) + \delta\psi(\mathbf{x}, t)$. The condensate part satisfies:

$$i\dot{\psi}_c = \frac{\lambda}{8m^2}|\psi_0|^2\psi_c\,, \tag{58}$$

that has a simple period solution $\psi_c(t) = \psi_0 e^{-i\mu_c t}$, where $|\psi_0|^2 = n_0$ is the number density of particles and fixes the amplitude of ψ_0, and $\mu_c = \frac{\lambda n_0}{8m^2}$. The phase of ψ_0 is arbitrary and any choice of it will spontaneously break the U(1) symmetry.

For the perturbation, we have, making the field redefinition $\psi = \psi_c\Psi$:

$$i\delta\Psi = -\frac{1}{2m}\nabla^2\delta\Psi + \frac{\lambda n_0}{8m^2}\left(\delta\Psi + \delta\Psi^*\right)\,. \tag{59}$$

Since Ψ is a complex scalar field, we can decompose the field into a real and a imaginary parts, $\Psi = A + iB$. We want to determine the dispersion relation of this system, so we Fourier transform the field and the equation of motion is now given as:

$$\frac{d}{dt}\begin{pmatrix} A_k \\ B_k \end{pmatrix} = \begin{pmatrix} 0 & \frac{k^2}{2m} \\ -\frac{k^2}{2m} - \frac{\lambda n_0}{4m^2} & 0 \end{pmatrix}\begin{pmatrix} A_k \\ B_k \end{pmatrix} . \tag{60}$$

The dispersion relation is given by:

$$\omega_k^2 = \frac{k^2}{2m} + \frac{\lambda n_0}{4m^2} . \tag{61}$$

For $\omega_k^2 > 0$ we have an oscillatory solution:

$$\delta\Psi_k = Z\left(\zeta_k - \omega_k^2\right) e^{i\omega_k t} + Z^*\left(\zeta_k + \omega_k^2\right) e^{-i\omega_k t} , \tag{62}$$

where $\zeta_k = (k/2m)\omega_k$. When $\omega_k^2 < 0$, the solution of the equation for $\delta\Psi_k$ is given by exponentials:

$$\delta\Psi_k = c_1\left(\gamma_k - i\omega_k^2\right) e^{\gamma_k t} + c_2\left(\gamma_k + i\omega_k^2\right) e^{-\gamma_k t} , \tag{63}$$

where $\gamma_k = (k/\sqrt{2m})\sqrt{-\omega_k^2}$ are the eigenvalues of the matrix, and c_1 and c_2 are constants given by the initial conditions. This shows us the when

$$\omega_k^2 < 0 \qquad \Longrightarrow \qquad k^2 < -\frac{|\lambda| n_0}{2m} , \tag{64}$$

there is an exponential growth of the perturbation. But this depends on the value of the interaction:

$$\begin{cases} \lambda > 0\,(\text{repulsive}) & \Longrightarrow \text{Stability} \\ \lambda < 0\,(\text{attractive}) & \Longrightarrow \text{Instability} \end{cases} \tag{65}$$

We can see that for a repulsive interaction, the homogeneous configuration is stable. However, for an attractive interaction, there is a stability for certain wavelengths, bellow which the is an instability, a parametric growth of perturbations, and thermalization will not be possible. In this case, a condensate with a long-range coherence is not guaranteed and the coherence length of the condensate depends on the size of the wavelength where the instability sets in. For the QCD axion, for example, $\lambda < 0$. So a condensate will be present on scales smaller than the wavelength that separates the stability and instability behavior.

Occupancy number evolution. With those solutions in hand, we can understand how the evolution of the occupancy number for the condensate will behave for each mode. This is given by: $n_k = |\psi_k|^2/V$, where ψ_k is constructed from the exponential and oscillatory solutions described above, with a random phase. The average occupation number evolves as:

$$\begin{aligned} \langle n_k(t)\rangle &= \langle n_k(t_i)\rangle \left\{1 + \tfrac{1}{2\gamma_k}\left(\tfrac{\lambda n_0}{4m^2}\right)\sinh^2\left[\gamma_k\left(t - t_i\right)\right]\right\} , \qquad \text{for } \omega_k^2 < 0 \\ \langle n_k(t)\rangle &= \langle n_k(t_i)\rangle \left\{1 + \tfrac{1}{2\omega_k}\left(\tfrac{\lambda n_0}{4m^2}\right)\sin^2\left[\omega_k\left(t - t_i\right)\right]\right\} , \qquad \text{for } \omega_k^2 > 0 \end{aligned} \tag{66}$$

For $\lambda > 0$, an repulsive interaction, γ_k is imaginary, and the hyperbolic sine becomes a sine: $((1/\gamma_k)\sinh^2\left[\gamma_k\left(t - t_i\right)\right] \to (1/\omega_k)\sin^2\left[\omega_k\left(t - t_i\right)\right])$, so the occupation number oscillates and the oscillations are stable. The ratio $\langle n_k(t)\rangle/\langle n_k(t_i)\rangle$ which has the largest value is obtained for modes that minimize $\omega_k \sim 1/k^2$. These are the longest wavelengths $k = 0$. So, the condensate is dominated by long-range correlations is stable.

For $\lambda < 0$, an attractive interaction, the occupation number grows exponentially. The fastest growth is given by the modes $k = k_*$ that maximize γ_k. So the modes $k > k_*$ or $\lambda < \lambda_*$, where $*$ denotes the characteristic scale where instability sets in, will dominate and the stable configuration of the system will be localized clumps. The size of these clumps will be given by the mass and interaction of the model. We describe these configurations next.

Ground state condensate solutions: Soliton. When $\lambda < 0$, the condensate is not a homogeneous long-ranged object, but a localized clump. Here we describe the condensate in the case of the self-interacting BEC. This configuration in this case is called *soliton*.

We can define the scale where instability starts by the k_* where the dispersion relations (61) is zero, $\omega^2_{k=k_*} = 0$. This scale is given by:

$$k_* = \sqrt{\frac{|\lambda|\, n_0}{4m}}\,. \tag{67}$$

For $k < k_*$ ($\lambda > \lambda_*$) parametric resonance sets in and structures should grow. The condensate cannot maintain coherence in this case, so there is no condensate on these scales. For $k > k_*$ ($\lambda < \lambda_*$), the solution oscillates and is stable, forming a condensate, the soliton. The soliton solution is stable in $1+1$ dimensions. In $3+1$ dimensions a phase transition happens and the soliton is not completely stable.

It is interesting to see that the size of this superfluid core is determined by the mass and the interaction parameter. For the QCD axion, usually $\lambda_a = -\Lambda^4/f_a^4$ is negative, so it will form these solitons. The interaction is extremely small, $\lambda_a \sim -10^{-48}$, because $\Lambda \sim 0.1$GeV, the typical QCD scale, and $f_a \sim 10^{11}$GeV, for typical Peccei-Quinn scale. The mass of the axion is approximately $m \sim 10^{-5}$eV. So the soliton length, for $n_0 \sim n_{gal}$, is $\lambda_s \sim 2.8\times 10^{11}\text{km} \sim 9\times 10^{-6}\text{kpc}$, which is much smaller than a galaxy, it is more a localized object. This means that the axion cannot be thought as a model for the condensate DM that has a wave behavior on galactic scales [118] .There are some analysis in the literature that reach a different conclusion [115–117], although not doing such a careful analysis.

One should note that even in the case of attractive interaction, if the mass is very small and/or the coupling is very small the ground state is homogeneous and given by long but finite wavelengths.

Ultra-light DM: Gravity

We are now going to describe a model without interaction but in a trapping gravitational potential. We are going to see that in this case, the gravitational potential is going to make the role of an attractive interaction. Counteracting the gravitational collapse, there is a quantum pressure, as seen in in eq. (54).

Evolution around the condensate and stability. The Schrodinger equation for DM in a gravitational potential, in the absence of interaction, is:

$$i\dot{\psi} = -\frac{1}{2m}\nabla^2\psi + m\Phi\psi\,, \tag{68}$$

which is coupled to the Poisson equation:

$$\nabla^2\Phi = 4\pi G\left(m|\psi|^2 - \bar{\rho}\right)\,, \tag{69}$$

where the average background density, $\bar{\rho}$, was subtracted. Expanding the field as done previously $\psi(\mathbf{x},t) = \psi_c(t) + \delta\psi(\mathbf{x},t)$, the equation for the condensate is trivial and $\psi_c = \psi_0 = \text{const.}$. For the fluctuations we can write the linearized systems of equations:

$$i\dot{\delta\Phi} = -\frac{1}{2m}\nabla^2\delta\Psi + m\Phi\,, \tag{70}$$

$$\nabla^2\Phi = 4\pi G\, m\, n_0\left(\delta\Psi + \delta\Psi^*\right)\,. \tag{71}$$

This can be combined into the equation:

$$i\dot{\delta\Phi} = -\frac{1}{2m}\nabla^2\delta\Psi + 4\pi G m^2 n_0\nabla^{-2}\left(\delta\Psi + \delta\Psi^*\right)\,. \tag{72}$$

One can notice that the equation above is very similar than the equation we had for the interacting case (59) for $\lambda/(8m^2) \leftrightarrow 4\pi G m^2\nabla^{-2}$. So, the theory of a trapped BEC or an axion field with an external gravitational potential can be though as a weakly interacting BEC theory, with an attractive interaction.

With that, we expect that there is an instability for long-range, and the condensate only be stable for a localized core with size given by the parameters of the potential and the mass. To determine this lets take the Fourier transform of the fields. Like in the interacting case, the instability is divided by the regimes where an analogous quantity to ω_k from (61), is smaller or bigger than zero. For the parameters in our case, I will call it $\tilde{\omega}_k^2$, and we determine the wavenumber that separates the regimes as:

$$\tilde{\omega}_k^2 = 0\,, \qquad \Longrightarrow \qquad k_J = \left(16\pi G m^3 n_0\right)^{1/4}\,. \tag{73}$$

This scale is the Jeans scale and it separates the regimes where gravity dominates and collapse happens ($k < k_J$); and the regime where the quantum pressure dominates and the solution is stable and oscillates ($k > k_J$). In this regime we can have a condensate. This quantum pressure that counteracts the gravitational attraction arises from the *uncertainty principle*: any attempt to localize the particle is accompanied by an increase in energy. So stability bellow the Jeans scale arises because of the uncertainty principle. The Jeans scale is the geometric mean of the the dynamical scale, defined in Section 2, and the Compton scale $\lambda_c = h/(m\,c)$.

We can estimate the size of the coherent condensate core. Rewriting the Jeans wavelength as:

$$\lambda_J = \frac{2\pi}{k_J} = \frac{\pi^{3/4}}{2}\left(G\rho\right)^{-1/4} m^{-1/2} = 55\left(\frac{m}{10^{-22}\mathrm{eV}}\right)^{-1/2}\left(\frac{\rho}{\bar{\rho}}\right)^{-1/4}\left(\Omega_m h^2\right)^{-1/4}\mathrm{kpc}\,, \tag{74}$$

where $\bar{\rho} = 2.8\times 10^{11}\,\Omega_m h^2 M_\odot \mathrm{Mpc}^{-3}$ is the background density. For *fuzzy DM*, we can see that the Jeans wavelength is of order 55kpc, forming a condensate on galactic scales. For the QCD axion, $\lambda_J \sim 1.7\times 10^{-7}$kpc, which is a very small scale in comparison to galaxies, forming a condensate of the size of very localized objects. This stable bound system is called a Bose star.

To describe a more complete scenario, we can add expansion. Continuing from (48), we can see that the system of equations is:

$$\frac{i}{a^{3/2}}\partial_t\left(a^{3/2}\psi\right) = -\frac{1}{2m}\frac{\nabla^2\psi}{a^2} + m\Phi\psi\,, \tag{75}$$

$$\nabla^2\Phi = 4\pi G a^2\left(m|\psi|^2 - \bar{\rho}\right)\,. \tag{76}$$

Like before, we calculate the linearize equations for the perturbations $\delta\Psi$ around the coherent homogeneous background that evolves as $\psi_c \propto a^{-3/2}$. Making this and combining the equations, we have that the equation for the perturbations is:

$$i\delta\dot{\Phi}_k = -\frac{k^2}{2ma^2}\delta\Psi_k - \frac{3}{2}m\Omega_a\frac{H^2a^2}{k^2}\left(\delta\Psi_k + \delta\Psi_k^*\right)\,, \tag{77}$$

where $\Omega_a = mn_0/\rho_{tot}$. Again, separating the real and imaginary part of perturbations, we have that the real part obeys:

$$\ddot{A}_k + 2H\dot{A}_k - \frac{3}{2}\Omega_a H^2 A_k + \left(\frac{k^2}{2ma^2}\right)^2 A_k = 0\,. \tag{78}$$

Added to the usual terms that are present for the usual CDM calculation, the last term of this equation is the quantum pressure. This arises from the uncertainty principle that can be seen from tracking the de Broglie wavelength of the light field. The Jeans length in this case is given by:

$$\frac{k_J}{a} = \left(6\Omega_a\right)^{1/4}\sqrt{Hm}\,. \tag{79}$$

4.1.1. Fuzzy Dark Matter

We studied above the evolution of a light scalar field behaving as DM in the presence of an interaction and under the influence of the gravitational potential. At late times, the dominant interaction is given by gravity, so it is natural to study the light scalar field in the absence of interaction. As we saw, in this regime the stability bellow the Jeans scale arises because of the uncertainty principle. In the case of *fuzzy DM* (FDM), the interest is that the condensate arising from this quantum pressure is of galactic scales in order to modify the dynamics on galactic scales and address the small scale problems of the ΛCDM. The calculation from last section shows that, since gravity is attractive, given the instability of the solution, in order to have a Jeans length of order o galaxies we need a very small mass, much smaller than the QCD axion mass.

In this section we will show the ranges of masses that give an attractive model for DM, and the astrophysical consequences of it. We show how these change the predictions from ΛCDM and the bounds that they might put in the parameters of the description [114][12].

Astrophysical and cosmological bounds in the FDM model. In this subsection we will show the bounds in the parameters of the models in order to be able to describe a good DM candidate. From the discussion above, we saw the there is an upper bound for the mass in order to condensate in galaxies (just condensate, no matter the size of the condensate) of $m \lesssim 4.7\text{eV}$ for a typical galaxy with $\rho_{gal} \sim 10^9\text{eV/cm}^3$ and velocity $v \sim 10^{-3}$. Later we saw that, for masses of order of the usual QCD axion mass, around $m \sim 10^{-5}\text{eV}$, the stable configurations are very localized and far from galactic scales, with that we can say that the upper bound in the mass is $m \ll 10^{-5}\text{eV}$. Now, we are going to see other conditions that can bound the mass and show the mass range that gives the best DM phenomenology.

Cosmological constraints: As we calculate above, the Jeans wavelength given by the fuzzy DM model is:

$$\lambda_J \simeq 70 h^{-1/2} \left(\frac{m}{10^{-22}\text{eV}}\right)^{-1/2} \text{kpc}\,. \tag{80}$$

The Jeans length in our case is not only the scales that divide the growth of structure, it also divides the behavior of DM: for $\lambda < \lambda_J$ there is no structure formation and the solution oscillates, and the fuzzy DM is in the condensed regime; for $\lambda > \lambda_J$ there is structure formation and the fuzzy DM does not behave as a condensate anymore, but as normal CDM.

Very roughly for the ultra-light DM to be important on galactic scales and suppress small scale structure formation on astrophysical scales, the mass of the ultra-light particle needs to be $m \lesssim 10^{-20}\text{eV}$. This comes by requiring that $\lambda_{dB} > \mathcal{O}(\text{kpc})$. So, we are going to study the influence of masses smaller than that. For those masses, the Jeans wavelength, from (80), is $> 70 * 10^2 h^{-1/2}$. The modes smaller that the Jeans length are going to oscillate and not produce structures. So for smaller and smaller masses, the scales that are suppressed are closer to the scales of cosmological interest and can be excluded by current cosmological data, since they will predict a very different power spectrum. In [125], the authors investigated that using CMB data from the Wilkinson Microwave Anisotropy Probe (WMAP), Planck satellite, Atacama Cosmology Telescope, and South Pole Telescope, as well as galaxy clustering data from the WiggleZ galaxy-redshift survey. With that, as we can see in Figure 3, they concluded that given this suppression, the mass of the ultra-light field needs to be

$$m \gtrsim 10^{-24}\text{eV}\,, \tag{81}$$

in order to be the dark matter and to reproduce the observations. Models with this mass range are going to be indistinguishable of CDM on large scales, which is what we wanted. If $m \lesssim 10^{-32}\text{eV}$ the ultra-light field can behave as dark energy.

[12] In this article [114] they use the word soliton to describe the condensate core in the inner regions of the galaxy. In the previous section we used this for the stable ground state solution of the interacting case, while we used the term Bose star for the ones formed by the presence of a gravitational potential. This is usually used in the literature interchangeably.

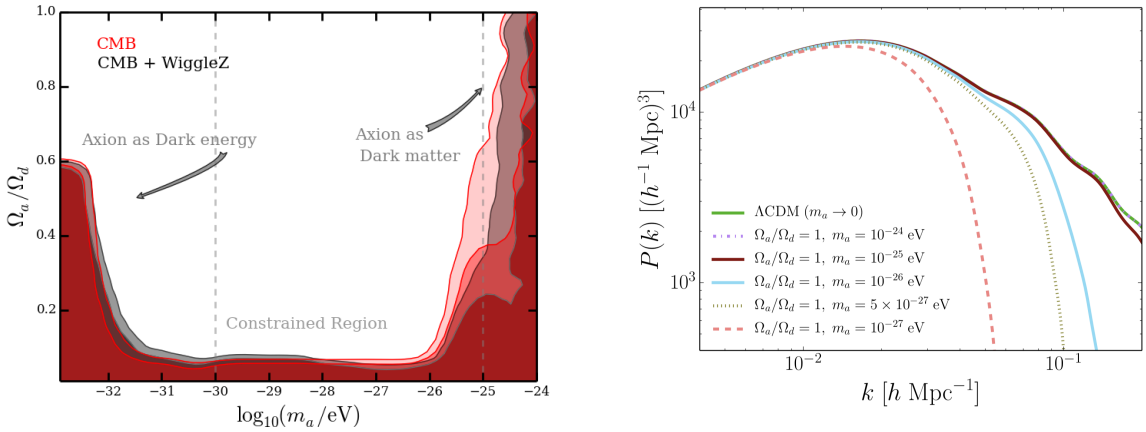

Figure 3: Figure from [125]. *Left panel:* that shows the 2σ and 3σ of the mass fraction $\Omega_{ultra-light}/\Omega_d$ in function of mass. The regions show the constrained region $\Omega_{ultra-light}/\Omega_d \lesssim 0.05$ at 95%, where Ω_d is the total dark-matter density fraction. Red regions show CMB-only constraints, while grey regions include large-scale structure data. *Right panel:* Adiabatic matter power spectrum for different ratios of masses of the ultra-light field.

This suppression of the power spectrum on small scales also suppresses the formation of galaxies. It is found in simulations that the number of subhalos in FDM in comparison to CDM is reduced by a factor of $\sim (3M/M_{1/2})^{2.4}$. This suppression of formation of small galaxies is larger in FDM at higher redshifts, in comparison to CDM. This opens up an important question about FDM being able to produce small scales structures at early times to be probed by Lyman-α forest.

Halos: minimum size, maximum density and the cusp-core problem One limit to the size of the condensed core is that it needs to be smaller than the virial radius, $\lambda_{dB} < R = GM/v^2$. This gives the maximum size for the condensate core: $R \gtrsim \frac{1}{GMm^2}$, where M is the mass of the galaxy. We can write that in terms of the radius where half of the mass of spherically symmetric of the system:

$$R_{1/2} \gtrsim 0.335 \left(\frac{10^9}{M_\odot}\right)\left(\frac{10^{-22}}{m}\right)^2 . \tag{82}$$

This bounds coincide with the measured from 36 Local group dwarf spheroidals [128] for a mass of $m \sim 10^{-22}$eV.

With the above condition, we can also compute upper bound in the central density:

$$\rho_c \leq 7.05 M_\odot \mathrm{pm}^{-3} \left(\frac{10^9}{M_\odot}\right)^{-4}\left(\frac{10^{-22}}{m}\right)^{-6} . \tag{83}$$

If we compare this bound to the observations from 8 dwarf spheroidals, we can see it is compatible if $m = 8^{+5}_{-3}\times10^{-23}$eV for Draco and $m = 6^{+7}_{-2}\times10^{-22}$eV for Sextans [129]. For those masses, the distribution at the center of the galaxies seem to be cored, alleviating the cusp-core problem. So, taking a fiducial mass of $m \sim 10^{-22}$eV seems to be in accordance to observations and to give observational consequences for DM in galaxies.

Lower bound on the FDM halo masses and the missing satellites problem As we saw before, for the self-gravitating FDM systems supported by quantum pressure, since gravity is attractive we have coherence on small scales. The size of this core depends on the mass, being larger as the mass is smaller. So the smallest radius to be produced in the FDM model are determined by the mass of the particle. This must have important cosmological consequences in the abundance of low mass halos,

in comparison with ΛCDM. We can see that by calculating the smallest structures formed in the FDM model. This is given by when $k = k_J$, which gives a Jeans mass:

$$M_J = \frac{4\pi}{3}\rho\left(\frac{1}{2}\lambda_J\right)^3 = 1.5\times10^7 M_\odot(1+z)^{3/4}\left(\frac{\Omega_{FDM}}{0.27}\right)\left(\frac{H}{70\text{km/s/Mpc}}\right)^{1/2}\left(\frac{10^{-22}}{m}\right)^{3/2}. \quad (84)$$

This is the minimum mass of substructure created in the FDM model. This is in contrast with CDM, where halos with mass bellow $\sim 10^{18}M_\odot$ are highly created, with abundance $dn(M_h) \propto M_h^{-2}dM_h$. In that sense, the missing satellites problem is reduced or resolved in the FDM model, since halos of smaller masses are not created. We are going to see bellow that tidal disruption can also act suppressing small mass haloes, aiding FDM in solving the missing satellites problem. The too-big-to-fail problem is also addressed by the FDM, since we have a mechanism to explain the fact that low-mass subhalos are not formed, we do not need to invoke mechanisms that create the too-big-to-fail problem.

Maximum soliton mass: Since this self gravitating system produces localized cores, we can find the maximum mass for a FDM soliton in an analogous way as the Chandrasekar mass for self-gravitating fermion system. We can estimate is as: $M_{max} = 0.633\hbar c/(Gm) = 8.46\times10^{11}M_\odot\left(10^{-22}\text{eV}/m\right)$. If self-interaction was considered, this mass would have been smaller. This is the maximum mass of the soliton, but the FDM model can contain bigger halos, where the the central core is only a fraction of the total halo mass.

Astrophysical consequences of FDM. Here we show some of the astrophysical consequences of the fuzzy DM model, with the parameters constraint by the criteria above.

- **Dynamical Friction**: An interesting puzzle is that of Fornax globular clusters. From dynamical friction it is expected that globular clusters orbiting Fornax should have rapidly fall towards its center to form a stellar nucleus. However, there is no signal of mergers and we detect 5 globular clusters orbiting Fornax.

  It is interesting to see how dynamical friction behaves in the presence of a condensate core. It is expected that the FDM changes this prediction because of three phenomena: (i) change in the rate of orbital decay because of the presence of the condensed core; (ii) since the FDM produces a homogeneous core, a mechanism similar to the "core stalling" observed in N-body simulations can take place and reduce or eliminate drag from dynamical friction; and (iii) the way dynamical friction is calculates must be modified by the presence of an object with large de Broglie wavelength, an quantum mechanical extension to the calculation of dynamical friction must be done. In [114] they describe only the last effect and simulate for different parameters the orbital decay times for Fornax in CDM and in the fuzzy DM cases. They found that in FDM the orbital decay time is longer, and four of the five decays times simulates are bigger than 10Gyr or more, thus explaning the puzzle for why the globular cluster in Fornax survived. Need more simulations and obervations to confirm this, but the fuzzy DM model seems to address the dynamical friction puzzle.

- **Most massive halos - clusters:** For distances larger than the de Broglie wavelength of the FDM, it is expected that DM behaves as standard CDM and that tha halo enveloping the soliton has a NFW profile. This can be seen numerically for the mass range $10^9M_\odot \lesssim M_{vir} \lesssim 10^{11}M_\odot$ [130–133], which gives an estimate for the mass of the central soliton. Extending relation to larger halos, FDM predicts that in the center region of clusters, there will be a condensed core, a soliton, with mass:

$$M \simeq 1.3\times10^{10}M_\odot\left(\frac{10^{-22}}{m}\right)\left(\frac{M_{vir}}{10^{15}M_\odot}\right)^{1/3}. \quad (85)$$

which is still bellow the maximum mass for the soliton calculated above. The corresponding half-mass radius is:

$$r_{1/2} \simeq 25\,\mathrm{pc}\left(\frac{10^{-22}}{m}\right)\left(\frac{M_{vir}}{10^{15}M_{\odot}}\right)^{-1/3}. \tag{86}$$

So, the presence of this soliton with this mass and size would be a prediction of the FDM model. But a question that remains to be answered is: in the presence of such solitons in the interior of clusters halos is in accordance to cluster mergers like the Bullet cluster or the anit-Bullet cluster?

In [114] they ask the question if solitons in the center of the galaxies are not been misinterpreted as super massive black holes. They compare the mass of the central dark region measured from Virgo and show that this is similar to the mass of the soliton core in a galaxy like Virgo for a mass of $m \sim 10^{-22}$. However, since the observation of the Event Horizon Telescope of the black hole in the center of M87, this hypothesis seem to be almost excluded, and it is indeed a super massive black hole. We have to wait for more data to confirm this.

Another interesting fact is that we know that the galaxies host a super massive black hole in its center. In [114] they investigate the possibility of a super massive black hole to be created in the center of a soliton. Apparently, the black holes do not grow for the fiducial mass, in a condensate core. Their creation only starts being significant for $m \gtrsim 5 \times 10^{-22}$eV, which is in tension with other bounds in the mass, like the one to solve the missing satellites problems.

- **Lyman-α constraints on FDM:**

  Recent investigation of FDM models in light of Lyman-α forest finds new constraints on FDM model parameters [134]. It puts a bound in the mass of FDM in the case where more than 30% of the DM being composed by this scalar field of $m \gtrsim 10^{-21}$. This value is larger than the value used for the FDM and is in tension with some of the predictions of the FDM model, like the ones necessary to solve the small scale problems of the ΛCDM.

  Lyman-α forest is an important probe of the matter spectrum on small scales, of order $0.5\mathrm{Mpc}/h \lesssim \lambda \lesssim 100\mathrm{Mpc}/h$. It is produced by the absorption seen in the light from quasar caused by the inhomogeneous distribution of neutral hydrogen in galaxies along different line of sights.

  In this work, they use data from the XQ-100 survey, 100 medium resolution spectra with emission redshift $3.5 < z < 4.5$. This data is compared against a simulation of the FDM with different masses and abundance today. On non-linear scales, quantum pressure is added. The result is shown in Figure 4. In the right panel of this figure we also see the impact of the constraints obtained in cosmology and in the astrophysical implications. In cosmology, the constraints obtained give a bound in the value of the displaced field, assuming that the genesis mechanism for this light field is vacuum displacement. Combining this data with CMB data, they also derive bounds on inflation, more specifically on r the tensor to scalar ratio for an inflationary epoch in the presence of FDM. They also show how this bound impacts the resolution of the small scale problems presented by FDM. The cyan line indicates the bound where the missing satellites problem is solved by FDM. The constraint is very tight and it shows a tension with the Lyman-*alpha* measurements.

  A possible caveat from this analysis is that they use hydrodynamical simulations, and they neglect quantum pressure. However, quantum pressure can be very important and play a vital role in structure formation, which is what the analytical behavior seems to show us [135].

- **Numerical simulations:** One of the biggest strengths of the FDM model is the amount of simulations that exist (see [136] for a review of the methods and simulations). Simulations are of extreme importance to constrain the parameter space of the model and to look for predictions of the theory. The simulations use one of the two approaches to describe the FDM system: the Schrodinger Poisson equation or the Mandelung equations.

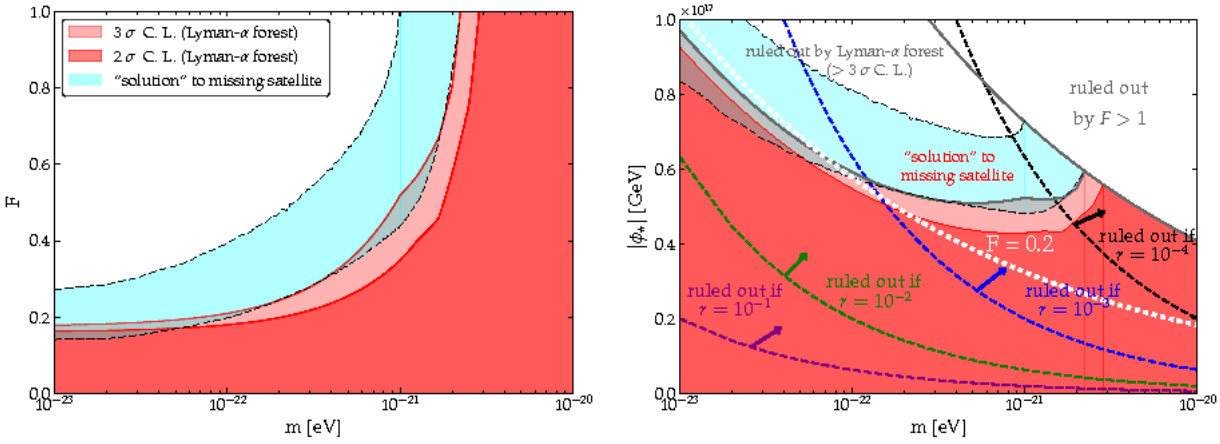

Figure 4: Figure from [134]. *Left panel:* Shows the constraint on the mass of the FDM and the fraction of the total DM mass from Ly-*alpha* forest measurements. *Right panel:* Constraints in the mass of the FDM and the value of the displaced field. This is combined with cosmological constraints, shown by the dashed lines for different tensor to scalar ratios. The cyan region is the region where the missing satellites problem can be solved by the FDM. The white dotted contour represents the line where FDM constitutes only 20% of the total DM.

With those simulations it is possible to investigate the phenomena above, and also to look for predictions that come from the quantum mechanical characteristic of these systems. For a review of some of the current status of simulation, see [136]. This is the new frontier for the description of these models and there is a lot of excitement for its results.

4.2. DM Superfluid

In this section we are going to describe the model of DM superfluid in details. In previous sections we saw the small scale problems of ΛCDM and how MOND empirical law offered a very good fit to the rotation curves of galaxies and the scaling relations that emerge from the dynamics of galaxies, which might be challenging in the context of ΛCDM. However, as we saw there is no present framework that can explain MOND, given that the initial proposed theory, the full MOND, and its extensions present serious problems. We present here an alternative model to DM that has the goal of reconciling CDM and MOND: the DM superfluid. In this framework, DM behaves as standard CDM on large scales, while the MOND dynamics emerges on galactic scales. This is possible through the physics of superfluidity.

On galactic scales, DM will go through Bose Einstein condensation and, given the interactions of these particles, form a superfluid core with coherent length of galactic scales. At those scales, DM does not behave like individual particles anymore but is described by the collective excitations of the condensate, the phonons. The phonons play a key role of mediating a long-range force between baryons. The effective dynamics that emerges on those scales is a MOND dynamics.

In the following we will construct the DM superfluid theory showing first in which conditions DM condensates on galactic scales, then we will present the theory that describes this superfluid phase. With that in hand we can calculate the halo profile and rotation curves in order to compare with data and check the fit of the theory. We present how this model explain many astrophysical systems and possible predictions. After that we show the limits of validit of this description and its relativistic completion. We briefly describe how the cosmology works in this model.

4.2.1. Conditions for DM condensation

Before describing how the DM superfluid behaves inside galaxies, we need to determine in which conditions DM condensates into a Bose Einstein condensate in galaxies. As we saw in the previous section, two conditions need to be met for condensation: first, we need that all the particles are in a single

coherent quantum state, described by a single wavefunction of the condensate; a second condition is that the DM particles are in thermal equilibrium, in order to be described by a Bose distribution.

In this section we want to obtain a rough estimate of the bounds in the parameters of the model in order to obtain a condensate on galactic scales. For that, for simplicity, we use the criteria for weakly interacting gases.

Condensate wavefunction. In order for the particles to be in a sigle quantum coherent state of the condensate is that the de Broglie wavelength of the particles in the condensate must overlap in order to form the single wavefunction of the condensate. This happens when the de Broglie wavelength is larger than the interparticle distance of the condensate constituents:

$$\lambda_{dB} \sim \frac{1}{mv} > l = \left(\frac{m}{\rho}\right)^{1/3} \qquad \Longrightarrow \qquad m < \left(\frac{\rho}{v^3}\right)^{1/4} , \tag{87}$$

where the interparticle distance is defined as the radius of a sphere that corresponds to the volume per particle of the system. This gives a bound in the mass of the DM particle.

Since we want the density and velocity of the dark matter halo, we are going to take this bound at virialization. Like described in Section 2.1, from standard spherical collapse, this is given by:

$$\rho_{200} = 200\rho_{cr} \sim (1+z_{vir})^3\, 1.95\times 10^{-27}\mathrm{g/cm}^3\,, \qquad V_{200} \sim 85\left(\frac{M}{10^{12}M_\odot}\right)^{1/3}\sqrt{1+z_{vir}}\,\mathrm{km/s}\,, \tag{88}$$

where we derived these expressions assuming $H_0 \sim 70\mathrm{km\,s^{-1}Mpc^{-1}}$ and in relation to a halo mass of order of the MW one. This gives the bound:

$$m \lesssim 2.3\,(1+z_{vir})^{3/8}\left(\frac{M}{10^{12}M_\odot}\right)^{-1/4}\mathrm{eV}\,. \tag{89}$$

Taking $z_{vir} \sim 2$, for example, this bound means that for a fixed mass, sat $m \sim 2eV$, halos with mass of order of $10^{12}M_\odot$, will obey (87) and will be in the condensed phase. More massive halos, like the ones from clusters, will be then in the in the normal phase, where DM behaves like particles.

Thermalization. The second condition to form a condensate is that the particles are in thermal equilibrium. The condition to achieve thermal equilibrium is that the time scale of thermalization must be smaller than the time scale where dynamical processes happen in the halo, the dynamical time. If this condition is satisfied and thermal equilibrium is achieved, the condensate is coherent in the entire halo.

The time scale of thermalization if given by the inverse of the self-interaction rate, and the condition for thermalization is given by:

$$\Gamma \sim \mathcal{N} v_{vir}\rho_{vir}\frac{\sigma}{m} \lesssim t_{dyn}^{-1} = (3\pi/32G\rho)^{-1/2}\,, \tag{90}$$

where $\mathcal{N} \sim \frac{\rho_{vir}}{m}\frac{(2\pi)^3}{(4\pi/3)(mv)^3}$ is the Bose enhancement factor, which tells you that for boson, if a boson is already in the state, the probability to another boson to be in that state will be enhanced by a factor of $\mathcal{N}$. The dynamical time is taken here as the time it takes to a sphere of density ρ to collapse due to gravity. This condition gives a bound in the self-interaction cross section:

$$\frac{\sigma}{m} \gtrsim 0.3\left(\frac{m}{\mathrm{eV}}\right)^4\frac{\mathrm{cm}^2}{g}\,, \tag{91}$$

where we assumed $z_{vir} = 2$ and $M = 10^{12}M_\odot$. If we want that our self-interaction satisfies the merging-cluster bound [137–139], which is $\sim 1\mathrm{cm}^2/\mathrm{g}$, this gives another bound in mass of the superfluid: $m \lesssim \mathrm{eV}$.

From these conditions, we can obtain a few properties of the our DM superfluid condensate:

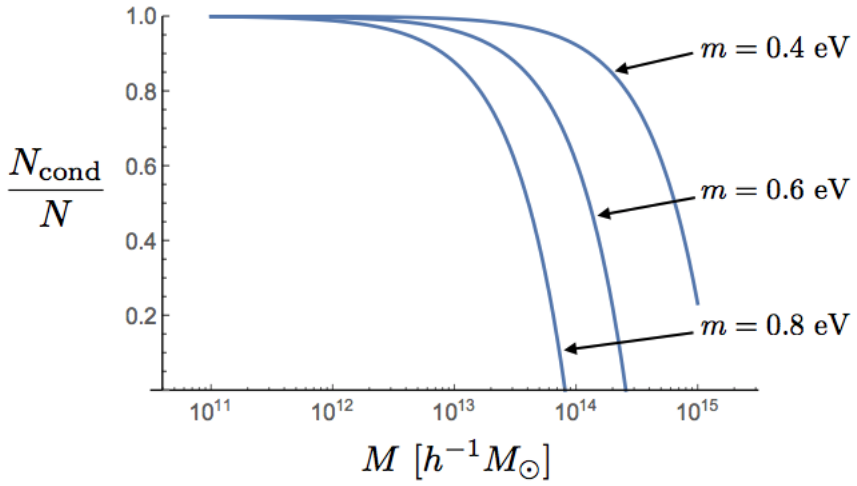

Figure 5: Approximate calculation form [121] for the fraction of the particles in the condensate versus in the normal state, for a series of sub eV masses in accordance with our bounds. We assumed $z_{vir} = 0$.

- **Critical temperature:** With DM is in thermal equilibrium, the temperature can be obtained by the equipartition theorem: $k_B T = m\langle v\rangle^2/2$, which is valid for temperatures smaller than the critical temperature. Above that temperature, equilibrium is broken and so does condensation. So, the critical temperature T_c is associated with the "critical" velocity v_c, than can be read when we saturate the bound (87):

$$T_c \sim 6.5 \left(\frac{\rm eV}{m}\right)^{5/3} (1+z_{vir})^2\,{\rm mK}\,. \tag{92}$$

  With that, the temperature in a given halo in units of T_c is given by:

$$\frac{T}{T_c} \sim 0.1(1+z_{vir})^{-1} \left(\frac{m}{\rm eV}\right)^{8/3} \left(\frac{M}{10^{12}M_\odot}\right)^{2/3} \tag{93}$$

- **Condensate fraction:** At $T = 0$ it is expected that almost all the particles are in the condensate. However, at finite but subcritical temperature, as seen in Landau's theory [88], it is expected that the fluid is going to be a mixture of superfluid and normal fluid, with the majority in the superfluid. As a back of the envelope calculation, this can be estimated as:

$$\frac{N_{cond}}{N} = 1 - \left(\frac{T}{T_c}\right)^{3/2} \sim 1 - 0.03(1+z_{vir})^{-3/2} \left(\frac{m}{\rm eV}\right)^4 \left(\frac{M}{10^{12}M_\odot}\right)\,. \tag{94}$$

  This formula is only valid for free-particles, and a particle with interaction and trapped in the gravitational potential has a different power than 3/2, but it serves as an estimate. We can in the Figure 5

The above conditions were obtained assuming that the condensate will take the entire halo. However, as mentioned in section 2.1, virialization occurs through violent relaxation, which is an out-of-equilibrium process. In this way, the DM superfluid cannot thermalize. What should happen is that first, the halo virialized and the profile is the expected NFW. After this process, DM particles start to enter thermal equilibrium in the inner, most central regions of the condensate, where the interaction is more pronounces. In this way, the halo would have am inner region ($r < R_T$) where DM is in a condensed state surrounded by the outer part of the halo ($r > R_T$) that follows the NFW profile [124]. Since in our model we want

to be able to describe the rotation curves of galaxies, R_T needs to be larger than the radius where the circular motion of stars and gas is observed. At this point, the density profile of the halo follows the NFW profile, $\rho \propto r^{-3}$. So we can rewrite the density and velocity with respect to the virial quantities used above: $\rho(r) = \rho(R_{200}\,(R_{200}/r)^3$, where for a NFW we can estimate $\rho_{200}/\rho(R_{200}) \sim 5$. With that, the thermalization bound becomes:

$$\frac{\sigma}{m} \gtrsim 0.2 \left(\frac{m}{\text{eV}}\right)^4 \left(\frac{M}{10^{12} M_\odot}\right)^{2/3} \left(\frac{r}{R_{200}}\right)^{7/2} \frac{\text{cm}^2}{g}\,, \tag{95}$$

which tells us that it is easier to reach thermal equilibrium in the center of the galaxies where the density is higher. This translates into a bound to the termalization radius:

$$R_T \lesssim 310 \left(\frac{m}{\text{eV}}\right)^{-8/7} \left(\frac{M}{10^{12} M_\odot}\right)^{1/7} \left(\frac{\sigma/m}{\text{cm}^2/g}\right)^{2/7} \text{kpc}\,. \tag{96}$$

For a MW-like galaxy with $M = 10^{12} M_\odot$ if we can measure the the curcular velocity up to approximately 60kpc, this will translate into a bound for the mass: $m \lesssim 4.2 \left(\frac{\sigma/m}{\text{cm}^2/g}\right)^{1/4}$eV. So estimated bounds for the conditions for virialization are also valid for the picture where the condensate is present in the center part of the galaxy.

4.2.2. Superfluid dynamics

Since we have determined that DM condenses and forms a supefluidity in the central regions of the halo, we now need to describe the evolution of this superfluid inside this region. We need to determine the dynamics of the superfluid in order to be able to calculate the profile of the region of the halo comprising the superfluid and with the calculate the rotation curves of galaxies. In this section we will describe the effective field theory of superfluids and show how this is theory reproduces MOND at small scales.

As we saw in the previous section, a superfluid at low-energies is described by the effective Lagrangian that is invariant under shift and Galilean symmetries:

$$\mathcal{L}_{T=0} = P(X)\,, \qquad X = \dot{\theta} + \mu - m\Phi - \frac{(\vec{\nabla}\theta)^2}{2m}\,, \tag{97}$$

where $\Phi = -GM(r)/r$ is the external gravitational potential for a spherical symmetric static source. The thermodynamic pressure is given by P.

We want our theory to describe the MOND dynamics at the regions where it is superfluid. Given this general Lagrangian for the phonons (97), we want it to describe the MOND action (6). For this, we conjecture that our phonon action is given by:

$$\mathcal{L}_{DM,T=0} = \frac{2\Lambda(2m)^{3/2}}{3} X\sqrt{|X|}\,. \tag{98}$$

This fractional power might seem strange from the point of view of a quantum field theory of fundamental fields, leading to superluminal behaviour and caustics. However, as a theory for the phonons this is not problematic and it determines uniquely the equation of state of the superfluid. As we can see for the condensate, where $\theta = \mu t$, setting the excitations and gravitational potential to zero, the pressure is given by the Lagrangian density:

$$P(\mu) = \frac{2\Lambda}{3}(2m\mu)^{3/2}\,, \qquad \Rightarrow \qquad P = \frac{\rho^3}{12\Lambda^2 m^6}\,, \tag{99}$$

where, in the non-relativistic regime, $\rho = mn$ and $n = \partial P/\partial\mu$ is the number density of condensed particles. As expected from the result from MOND, this Lagrangian gives us an EoS for the superfluid $P \propto \rho^3$, which is what we wanted to reproduce MOND.

The action for the phonons excitations ϕ can be obtained by expanding (97) to quadratic order. Neglecting the gravitational potential:

$$\mathcal{L}^{(2)} = \frac{(2m)^{3/2}}{4\mu^{1/2}} \left(\dot{\phi}^2 - \frac{2\mu}{m} (\vec{\nabla}\phi)^2 \right) , \tag{100}$$

from where we can infer the sound speed of the phonon excitations:

$$c_s = \sqrt{\frac{2\mu}{m}} . \tag{101}$$

One piece is missing in order to reproduce the MOND action in our framework. To mediate the MOND force, phonons have to couple to the baryon mas density:

$$\mathcal{L}_{int} = -\alpha \frac{\Lambda}{M_{pl}} \theta \rho_b , \tag{102}$$

where α is a dimensionless coupling constant. Although necessary in order to obtain the MOND regime, this interaction Lagrangian breaks shift symmetry, but softly, only at the $1/M_{pl}$ level. This term is here considered as a phenomenological term. In this way, this superfluid theory has 3 parameters: the mass m, the scale Λ and the coupling α.

The present form of the Lagrangian to obtain MOND is not the only way of obtaining the MOND behavior in the context of the DM superfluid model. In [122] he uses higher order corrections to generate the non-relativistic MOND action, which is inspired in the symmetron mechanism. Using the same Lagrangian (98) as the leading order Lagrangian, higher order corrections involving gradients of the gravitational potential are added to effectively modify the gravitational force. This results in the spontaneous breaking of a discrete symmetry. The symmetry is broken for small accelerations leading to MONDian gravity, and is restored in the limit of large acceleration leading to Newtonian gravity. In this theory the shift symmetry of the entire system is maintained. A difference from the present mechanism, as we are going to see is that cosmologically all the DM is in the normal phase, behaving like CDM, and reproducing all the results from ΛCDM. I will stick with the method of adding a photon-baryon coupling since this was studied in more detail.

Finite Temperature

The theory developed above is valid for a $T = 0$ superfluid. However, in reality, the DM in galaxies has a non-zero temperature. As we mentioned in Section 3, for finite temperatures, this Lagrangian needs to receive finite temperature corrections. Landau's model for a finite temperature superfluid consists in a mixture of superfluid component and a normal component. Those components interact with each other. At lowest order in derivatives, the general form of the EFT at finite temperatures and finite chemical potential is a function of three scalars [143]:

$$\mathcal{L}_{T\neq 0} = F\left(X, B, Y\right) , \tag{103}$$

where $X = X(\theta)$ was defined before with respect to the superfluid variables. The other new components are: B is defined with respect to the normal fluid three Lagrangian coordinates $\varphi^I(\vec{x}, t)$; and Y represents the scalar product of the normal and superfluid velocities:

$$B \equiv \sqrt{\det \partial_\mu \varphi^I \partial^\mu \varphi^I} , \qquad Y \equiv u^\mu \left(\partial_\mu \theta + m\delta^0_\mu \right) \simeq \mu - m\Phi + \dot{\phi} + \vec{v} \cdot \vec{\nabla}\phi , \tag{104}$$

where u^μ is the unit 4-vector from $\varphi^I(\vec{x}, t)$, and in the last equality of Y we have taken the non-relativistic limit, so $\vec{v}$ is the velocity vector of the normal fluid component.

There are many ways to construct the finite temperature operators. Our restriction is that we want our finite-temperature theory to generate the expected MOND profile. To construct such a Lagrangian

requires first-principle knowledge of the microphysics of the superlfuid. Since we still don't have a fundamental description of the DM superfluid theory, we proceed empirically. We suggest the following finite-temperature Lagrangian for the model:

$$\mathcal{L} = \frac{2\Lambda(2m)^{3/2}}{3} X\sqrt{|X-\beta Y|} - \alpha\frac{\Lambda}{M_{pl}}\phi\rho_b\,, \tag{105}$$

where β is a dimensionless constant that parametrizes the finite temperature effects. When $\beta \to 0$, we recover the $T = 0$ result; we are using the fiducial value $\beta = 2$. We included the interaction term so we could represent the entire action of the theory.

4.2.3. Halo profile

With the Lagrangian of the theory, we can evaluate the halo profile in the superfluid region and, after matching with an outer NFW profile, calculate the rotation curves of galaxies. And this is what we are going to do in this section: estimate the halo profile. This will be done in steps. First, we estimate the DM halo profile taking into account only the density coming from (98). Next, we include the baryons, by calculating the profile for the full action including interaction. We are going to use here the finite-temperature effective action (105), since in the case of the $T = 0$ analysis the perturbations around this zero-temperature static background are unstable, ghost-like. Although phenomenological, it retains the features of the initial superfluid Lagrangian and can give a more realistic description.

DM halo profile

With the equation of state (99) we can evaluate the density profile of the *condensate component* in the halo. First, we will calculate the DM halo profile in the absence of baryons.This is the halo profile given by the different equation of state that the superfluid give: $P \propto n^3$. This analysis is almost the same for the zero-temperature and finite temperature cases, with accounts for the replacement:$\Lambda \to \tilde{\Lambda} = \Lambda\sqrt{\beta-1}$. Assuming hydrostatic equilibrium, for a static spherically symmetric halo, the pressure and acceleration are related by:

$$\frac{1}{\rho(r)}\frac{dP(r)}{dr} = -\frac{d\Phi(r)}{dr} = -\frac{4\pi G}{r^2}\int_0^r dr^{'}\, r'^2\rho(r^{'})\,. \tag{106}$$

By making a change of variables $\rho(r) = \rho_0\Xi$ and $r = \xi\left[\rho_0/(32\pi G\tilde{\Lambda}^2 m^6)\right]^{1/2}$, where $\rho(r=0) = \rho_0$, this equation reduces to the Lane-Emden equation (with $n = 1/2$):

$$\frac{1}{\xi^2}\frac{d}{d\xi}\left(\xi^2\frac{d\Xi}{d\xi}\right) = -\Xi^{1/2}\,. \tag{107}$$

Choosing boundary conditions $\Xi(0) = 1$ and $\Xi^{'}(0) = 0$, we can numerically solve this equation. We can see from the change of variables that [**?**] the size of the condensate and the central density are given by:

$$R = \xi_1\sqrt{\frac{\rho_0}{32\pi G\tilde{\Lambda}^2 m^6}}\,, \qquad \rho_0 = \frac{M}{4\pi R^3}\frac{\xi_1}{|\Xi^{'}(\xi_1)|}\,, \tag{108}$$

where ξ is where the numerical simulation vanishes. From the numerics $\xi_1 \sim 2.75$ and $\Xi^{'}(\xi_1) \sim -0.5$ gives the following halo radius and central density:

$$\rho_0 \sim \left(\frac{M_{DM}}{10^{12}M_\odot}\right)^{2/5}\left(\frac{m}{\mathrm{eV}}\right)^{18/5}\left(\frac{\Lambda}{\mathrm{meV}}\right)^{6/5}(\beta-1)^{3/5}\ 10^{-24}\mathrm{g/cm}^3\,, \tag{109}$$

$$R \sim \left(\frac{M_{DM}}{10^{12}M_\odot}\right)^{1/5}\left(\frac{m}{\mathrm{eV}}\right)^{-6/5}\left(\frac{\Lambda}{\mathrm{meV}}\right)^{-2/5}(\beta-1)^{-1/5}\ 45\mathrm{kpc}\,, \tag{110}$$

With that, we can determine the chemical potential $\mu = \rho^2/\left(8\Lambda^2 m^5\right)$. We can see that $m \sim$ eV and $\Lambda \sim$ meV give realistic halo sizes, so we choose the fiducial values:

$$m = 0.6\text{eV}\,, \qquad \Lambda = 0.2\text{meV}\,. \tag{111}$$

For these values, the radius of the condensate core is 158kpc for $M_{DM} = 10^{12} M_\odot$. The condensate does not make the entire halo, but we expect that this condensed core is surrounded by a NFW profile. We will see this calculated in Section where we present the rotation curves. For those values we can also see that the density profile is *cored* and has a much smaller central density than the obtained in CDM simulations and more in agreement with observations. In this way the DM superfluid model offers a simple resolution to the cusp-core and the "too big to fail" problems.

Including baryons

Now, we want to include baryons so we can derive the proper phonon profile in galaxies. We expect that there is this extra acceleration due to the interaction to baryons. This comes from the dynamics of the phonon excitation ϕ given the the Lagrangian (105) We are going to assume a static, spherically symmetric approximation: $\theta = \mu t + \phi(r)$. The equation of motion for the phonon is given by:

$$\vec{\nabla} \cdot \left(\frac{(\vec{\nabla}\phi)^2 - 2m\hat{\mu}}{\sqrt{(\vec{\nabla}\phi)^2 - 2m\hat{\mu}}}\, \vec{\nabla}\phi \right) = \alpha \frac{\rho_b}{2M_{pl}}\,, \tag{112}$$

where $\hat{\mu} \equiv \mu - m\Phi$. If we ignore the homogeneous curls term, in the limit where $(\vec{\nabla}\phi)^2 \gg 2m\hat{\mu}$ the solution is:

$$|(\vec{\nabla}\phi)|\,(\vec{\nabla}\phi) \simeq \alpha M_{pl} \vec{a}_b\,, \tag{113}$$

where $\vec{a}_b$ is the Newtonian acceleration due to baryons only. Then acceleration mediated by ϕ is:

$$\vec{a}_\phi = \alpha \frac{\Lambda}{M_{pl}} \qquad \Longrightarrow \qquad a_\phi = \sqrt{\frac{\alpha^3 \Lambda^2}{M_{pl}}\, a_b} = \sqrt{a_0 a_b}\,, \tag{114}$$

for $a_0 = \alpha^3 \Lambda^2 / M_{pl}$, which is exactly the acceleration expected in the deep MOND regime, as showed in Section 2.3. In the regime $(\vec{\nabla}\phi)^2 \ll 2m\hat{\mu}$, we recover the Newtonian acceleration given by the baryons. So, in our case, the total acceleration is given by $\vec{a}_b$, $\vec{a}_\phi$, and also $\vec{a}_{DM}$ the Newtonian acceleration from the DM halo itself (obtained in the previous section), since we have DM in this model (different than MOND).

Halo profile algorithm

Having developed the theory of the superfluid DM above, now we want to evaluate the density profile of the DM halo and the rotation curves, and compare it with the data to make a first proof of concept of the model. To evaluate the rotation curve, we need to determine

As discussed in our model the galaxy contain a superfluid core in the central region of the galaxy surrounded by a NFW profile envelope. So in order to calculate these quantities for the galaxy we first need to evaluate them inside the superfluid core, and then at $R = R_{NFW}$ match the density and the pressure obtained for the superfluid ρ_{SF} and P_{SF}, to the ones given by the full NFW profile.

For that, we need to evaluate these quantities in the superfluid phase. In order to obtain the halo density profile, we need to determine the total mass of the halo $M(r)$. The rotation curve is the circular velocity with respect to the radius, given by $a = v_{circ}^2(r)/r$ where $a = \partial\Phi/\partial r$. So we need to determine the gravitational potential Φ in order to calculate the rotation curve and, also to determine $M(r)$. The Poisson equation in the superfluid region is given by:

$$\nabla^2 \Phi = 4\pi G\,(\rho_{SF} + \rho_b)\,. \tag{115}$$

Table 2: Summary of observational consequences of superfluid DM from [124].

System	Behavior
Rotating Systems	
Solar system	Newtonian
Galaxy rotation curve shapes	MOND (+ small DM component making HSB curves rise)
Baryonic Tully–Fisher Relation	MOND for rotation curves (but particle DM for lensing)
Bars and spiral structure in galaxies	MOND
Interacting Galaxies	
Dynamical friction	Absent in superfluid core
Tidal dwarf galaxies	Newtonian when outside of superfluid core
Spheroidal Systems	
Star clusters	MOND with EFE inside galaxy host core — Newton outside of core
Dwarf Spheroidals	MOND with EFE inside galaxy host core — MOND+DM outside of core
Clusters of Galaxies	Mostly particle DM (for both dynamics and lensing)
Ultra-diffuse galaxies	MOND without EFE outside of cluster core
Galaxy-galaxy lensing	Driven by DM enveloppe $\implies$ not MOND
Gravitational wave observations	As in General Relativity

The baryon density is given by the observations, while the superfluid density we can obtain from our theory. Differentiating our Lagrangian (105) with respect to the gravitational potential, we can obtain the superfluid density:

$$\rho_{SF} = \frac{2\sqrt{2}m^{5/2}\Lambda\left[3(\beta-1)\hat{\mu}+(3-\beta)\frac{(\vec{\nabla}\phi)^2}{2m}\right]}{3\sqrt{(\beta-1)\hat{\mu}+frac(\vec{\nabla}\phi)^2 2m}}\,, \tag{116}$$

where we can see that $\rho_{SF} = \rho_{SF}(\Phi, \phi)$. So, in order to solve the Poisson equation, we need the equation for ϕ, which is given by its equation of motion (112). The system of equations we need to solve is given by (115) and (112), which can be very intricate to solve. One approximation that can be done to simplify this is to assume that baryon distribution is spherically symmetric (which we know it is not true, but we use as a simplification). With that, we can solve the system numerically. This is done in [124]. After having this, we make the procedure of matching to NFW. With that, it is possible to evaluate the density profile and the rotation curves of galaxies.

4.2.4. Observational consequences

In this section we will describe the main observational consequences of the Superfluid DM. A summary of all the effects already worked out can be seen in Table 2. Since it is going to be used a lot in this section, just reminding Landau's conditions for superfluidity is that the fluid velocity (v_s) is smaller than the superfluid sound speed c_s, $v_s < c_s$.

- **Galaxy rotation curves:**

  In [124] the rotation curves of IC 2574, a low surface brightness galaxy, and UGC 2953, a high surface brightness galaxy, were numerically calculated using the method developed above, as a proof of concept of the galactic dynamics that the DM superfluid is able to reproduce. Since for the theoretical predictions a spherical baryonic distribution was assuming to simplify the calculations, this is far from the actual distribution. So, in these calculations it was hybrid method mixing the results calculated with the spherical distribution, corrected for the actual distribution leading to:

  $$\vec{a}_{hybrid} = \vec{a}_{b,real} + \vec{a}_{DM} + \vec{a}_{phonon}\,, \tag{117}$$

  where $\vec{a}_{b,real}$ is the acceleration computed from Poisson's equation for a non-spherical accelerations; $\vec{a}_{DM}$ the Newtonian acceleration from the DM halo using spherical baryon distribution; and $\vec{a}_{phonon}$

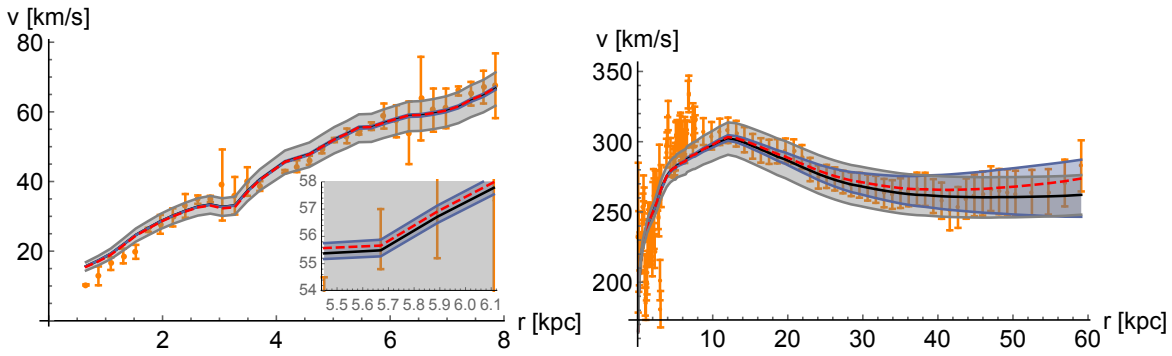

Figure 6: Predicted rotation curves evaluated in [124]. *Left panel:* Predicted rotation curve of IC 2574,a LSB galaxy. The orange points are data from [**?**] assuming a distance of 3 Mpc [144], the black and red curves are the predicted curves for $M_{DM} = 20M_b$ and $50M_b$. The gray band corresponds to two values of $a_0 \in (0.6, 1.2) \times 10^{-8}$ and the blue band two values of $\Lambda \sim (0.02, 0.1)$meV. *Right panel:* Rotation curve of UGC 2953. The orange points are data from [145] with all the parameters like in the Left panel figure, but the red curve where $M_{DM} = 65M_b$.

from (**??**) sourced by $\vec{a}_{b,real}$, but with Newtonian potential from the spherical case. Although calculated in the hybrid method, $\vec{a}_{phonon} \sim \sqrt{a_0 a_b}$ as expected in MOND regime.

The fiducial parameters used for this numerical calculation were $m = 1$eV, $(\sigma/m) = 0.01\,\mathrm{cm}^2/\mathrm{g}$, which are optimal for having a superfluid core that encompasses the baryonic disk of the galaxy, while still within the bounds to agree with cluster observations; $\Lambda m^3 = 0.05\,\mathrm{meV}\times\mathrm{eV}^3$; and $\alpha = 5.7$. The rotation curves can be seen in Figure 6.

1. *LSB galaxy:* As pointed out before since they are DM dominated, the rotation curves from LSB are expected to have a slow raise before reaching the plato region. As we can see in the *left panel* of Figure 6, our model reproduces the observed rotation curve for IC 2574, represented by the orange points, very precisely for the parameters chosen.
   The size of the superfluid core obtained for this galaxy is $R_{SF} \sim 40$kpc, which here is represented by the NFW radius where the profile is matched with a NFW profile and has a close value to R_T. Relative to $R_{200} \sim 57$kpc for this galaxy, the superfluid core is relatively large encompassing 58% of the total DM mass of the halo.
2. *HSB galaxy:* The rotation curve features of HSB galaxies are known to be hard to be reproduced. We saw that MOND empirical theory is successful in reproducing those features. It is interesting to see if our model is also able to reproduce it. The rotation curve for UGC 2953 is shown in the *right panel* of Figure 6, using the same conventions as for the LSB. The radius obtained for the superfluid core in this case is $R_{SF} \sim 79\,\mathrm{kpc}$, which is small in comparison to $R_{200} \sim 245\,\mathrm{kpc}$, encompassing 24% of the total DM mass. The difference from the LSB results is the red curve, where the total DM mass is set by the ΛCDM abundance matching value of $M = 65\,M_\odot$. For the red curve, we get a bigger superfluid radius, $R_{SF} = 93\,\mathrm{kpc}$, which is still significantly smaller than $R_{200} = 446\,\mathrm{kpc}$. The rotation curves seem to fit the data well, showing a smaller value but still compatible with observations for the velocity in the point where the curve turns to flat. Also, the superfluid DM show a slight rise in the end of the rotation curve, which is compatible to the data but not existent in MOND.

In general, it seems that the superfluid model reproduces the rotation curves of LSB and HSB galaxies. Also, the BRTF relation is also satisfied, as expected. Of course, this calculation shows a proof of concept and the rotation curves of many more galaxies with different characteristics need to be fitted, also to help determine the parameters of the theory, which were chosen here. However, we can already anticipate that we expect this to work for galaxies with very different masses, since

the phonon-baryon coupling guarantees this behavior for the rotation curve within the core; outside the core its is going to be very different.

- **Galaxy Clusters:** In a simple way, following the analyses in Section 4.2.1, clusters have large dispersion velocities, and at large distances, of order of R_{200}, $\mathcal{N}$ is going to be small and thermal equilibrium cannot be achieved. The DM in clusters is in the normal phase. However, as we saw for galaxies, in the central regions the density increases and thermal equilibrium may be achieved. In clusters only a very small amount can be in the superfluid state, since observations exclude that clusters are largely in the superfluid regime. We can then see the bounds in our mass in order to have a small amount of superfluid component in clusters that is not in tension with data. We assume that $R_T/R_{200} \lesssim 0.1$, which gives, using the relations from Sections 4.2.1 and 2.1:

$$R_T \lesssim 200 \left(\frac{M}{10^{15} M_\odot}\right)^{1/3} kpc\,. \tag{118}$$

  We can now repeat the analysis of thermal equilibrium done in Section 4.2.1. However, for such a small R_T in comparison to the cluster size, we use the full NFW profile. This yields a constraint in the mass of the DM particles:

$$m \gtrsim 2.7 \left(\frac{\sigma/m}{\mathrm{cm}^2/g}\right)^{1/4} \mathrm{eV}\,. \tag{119}$$

  This combined with the constraints from the thermalization in galaxies gives the allowed range for the DM mass:

$$2.7\mathrm{eV} \lesssim m \left(\frac{\sigma/m}{\mathrm{cm}^2/g}\right)^{-1/4} \lesssim 4.2\mathrm{eV} \tag{120}$$

  From the tightest constraints from approximately 30 merging systems [**?**], $\sigma/m \lesssim 0.5\mathrm{cm}^2/\mathrm{g}$. This value is in accordance with the one from Section 4.2.1, from the above constrain gives a DM mass between $1.5\mathrm{eV} \lesssim m \lesssim 2.4\mathrm{eV}$. For DM superfluid in this mass range, we have condensation inside galaxies and the condensation in the interior of cluster happens in very small radius, appearing not to be in conflict with what is expected from observations. This constraint can be made broader by assuming a more realistic a not constant cross section. A quantitative analysis via numerical simulations would be ideal to check this result.

- **Galaxy mergers:** The behavior of merging galaxies is an interesting question, given the superfluid nature proposed for the inner core of galaxies. But the existence of these superfluid phases in these merging systems is going to depend on the comparison between the infall velocity for the merging galaxy and the sound speed of the phonon, the Landau criteria.

  - $v_{infall} \gtrsim c_s$ - you will have the DM particles in the halo in the normal phase, since the halos were driven out of equilibrium, exciting the DM matter particles out of the condensate. The merging process will proceed as in ΛCDM, where dynamical friction leads to rapid merger. Thermal equilibrium and condensation will be achieved in the merged halo after some time.
  - $v_{infall} \lesssim c_s$ - In this regime, the halo DM in the superfluid phase, and the superfluid cores will pass through each other. In this case, dynamical friction is reduced taking a much longer time to the system to merge, and possible multiple encounters.

  In our case, the phonons have sound speed $c_s = \sqrt{2\mu/m}$, and for the fiducial values adopted (**??**), $c_s \sim 220\mathrm{km/s}$ for a $10^{12} M_\odot$ halo. This needs to be compared with the infall velocities of galaxies to see how the merger dynamics proceeds.

- **Merging Clusters: the Bullet and the Counter-Bullet:**

The Bullet cluster is one of the best evidences of the existence of DM (and against alternatives like MOND). This is seen by a segregation in the position of the mass peak (highest concentration of total matter) given by lensing that probes all the matter content, and the one from X-ray measurements, which measures the baryonic matter. This is consistent with the CDM picture, where the DM in the merging processes due to its negligible interaction passes through almost without interaction, while the baryons are slowed down. This poses a problem for theories that do not have DM.

The Bullet cluster can be explained in the context of the DM superfluid. As we saw above, like in galaxy clusters, the outcome of the merging depends on the infall velocities, but also in the amount of the components in each phase. If the infall velocities are subsonic, the halos are in the superfluid phase and they will pass through each other without friction. The normal component is slowed down due to self-interactions. In this way, the signal expected is a mass peak at the galactic center because of the superfluid component and another X-ray luminosity peak due to the normal component. These expected features are what it is measure for Abell 520 "train wreck" [146–149].

In the case of the Bullet cluster, in order to be consistent with observations, at least the sub-cluster must be in the superfluid phase. As we can see, the sound speed of the phonon for the sub-cluster ($M_{sub} \sim 10^{14} M_\odot$) is, for our fiducial values, $c_{s,sub} \sim 1400$km/s, while for the main cluster ($M_{main} \sim 10^{15} M_\odot$) is $c_{s,main} \sim 3500$km/s. The relative velocity between the clusters is ~ 2700km/s. [150, 151]. If we take this to be the infall velocity, we can see that the sub-cluster is in the superfluid phase, while the main cluster is in the normal phase. With that, dissipative processes between the superfluid cores should be suppressed and the bullet cluster is predicted as expected.

- **Dynamical Friction:** From the very definition of superfluidity, the absence of dynamical friction may lead to interesting astrophysical consequences and help understand some puzzles with CDM [114, 141].

  One example that can be explained by this characteristic of superfluids is velocity of galactic bars in spiral galaxies, which are expected to have been slowed down by dynamical, but are measured to be nearly constant which is consistent with no dynamical friction.

  An interesting puzzle is that of Fornax globular clusters. From dynamical friction it is expected that globular clusters orbiting Fornax should have rapidly fall towards its center to form a stellar nucleus. However, there is no signal of mergers and we detect 5 globular clusters orbiting Fornax. In the presence of a superfluid in the halo, given the absence of dynamical friction, these globular cluster should not necessary have merged with Fornax.

  There is also speculation that this absence of dynamical friction can lack of feature in the two-point correlation function of luminous red galaxies, consequences for the history of the Local Group, among others. The quantitative analyses of dynamical friction is currently under investigation.

- **Gravitational Lensing:**

  In the case of the full MOND theory,or its relativistic completion TeVes, the absence of DM to be able to explain makes it necessary the introduction of a complicated non-linear term between the scalar field of the theory and baryons, which should also couple to a time-like vector field in order to give the correct gravitational potential to be able to explain gravitational lensing.

  In the case of the DM superfluid, since the theory has DM, so we have the superfluid component described by the phonon scalar field, and we have the normal component which provides the time-like vector field u^μ. The gravitational potential is then sourced by both dark matter and baryons, as expected.

  As we have that the superfluid core resides in the inner part of the galaxy, surrounded by an NFW envelope, gravitational lensing will come primarily from this NFW outter part. This analyses deserves a more detailed analysis.

Recently, the DM superfluid model was studied in the context of strong lensing [156].

- **Gravitational waves:**

  In the superfluid DM, different than in MOND, there is no need to postulate any non-minimal coupling between to reproduce galaxy-galaxy lensing. So photons and gravitons propagate at the speed of light travelling along the same geodesics. This is in agreement with the recent constraints from the gravitational waves from neutron stars merger GW170817 [157], which rule out relativistic completions of full MOND [158].

  The implications for the gravitational waves in the case where the phonon has a non-vanishing sound speed was considered in [159], together with its observational effects in future GW experiments.

  Specifying the microphysics of the DM superfluid particle can also yield other signatures in the produced gravitational waves, like chirality, as done in [160].

Vortices and other quantum effects: "directly" probing the superfluid

Quantum vortices are a prediction of rotating superfluids and its measurements would be a smoking gun for the superfluid model. When rotated to velocities above a critical angular velocity, the superfluid develops quantum vortices that carry angular momentum. To calculate the abundance and properties of those vortices, it is necessary to have a full microscopic description of the superfluid. Since this is still missing in our model, here we present a dimensional analysis and order of magnitude analyses regarding the presence of vortices in our context.

Vortices are formed when the angular velocity of the superfluid is bigger than the critical velocity: $\omega_{Sf} \gg \omega_{cr}$. The critical angular velocity of a superfluid is given by[140]:

$$\omega_{cr} = \frac{1}{mR^2} \ln\left(\frac{R}{\xi}\right) . \tag{121}$$

For $R \sim 100$kpc and $m \sim$ eV, we can that $w_{cr} \sim 10^{-41}\mathrm{s}^{-1}$ (neglecting the logarithmic factor). This is much smaller than the rotation velocity of the halo: $\omega \sim \lambda\sqrt{G\rho} \sim 10^{-18}\mathrm{s}^{-1}$, where λ is called the spin parameter and from simulations is given by $0.01 < \lambda < 0.1$ and using a halo mass density $\rho \sim 10^{-25}\mathrm{g/cm}^3$. So, there will be the production of vortices in the halos of the galaxies.

And this production seem to be very numerous. We can estimate the number of vortices in the halo $N_v = \omega/\omega_{cr} \sim 10^2 3$, with a core radius, given by the healing length, $\xi = 1/(mc_s) \sim$ mm (assumed a MW type galaxy and fiducial values). Although highly numbered, these vortices are small. It is still unclear if it is possible to detect those vortices via, for example, gravitational lensing or any other effect they might have in the galaxy. This topic worth further investigation since the detection of such effect would be an important evidence for the presence of superfluids in galaxies.

Another interesting effect that come from the quantum nature of superfluids and that would be interesting to be observed is the interference patterns, fringes, caused by dark/bright solitons in the merging processes [153]. This effect was studied in the context of Dark/bright solitons are wave solutions of Gross Pitaevskii equation that preserve its shape through propagation and can have minimum or maximum density, respectively. This effect was studied for the case of BEC DM in [154], and it would be interesting to study it in the context of Superfluid DM in order to see if this effect would be yield observable consequences. A suggestion to be investigated is if this effect could be linked to the shells seen around elliptical galaxies [155].

4.2.5. Validity of the EFT

In this section we are going to scrutinize the validity of the EFT.

Higher Order Derivatives

First, we need to check if it is valid to ignore higher order terms in the EFT. As we saw above, the EFT is constructed by including all the terms which are invariant under shift symmetry. We retained only the first order contributions, given that we are working in the low-energy limit. Higher order terms involve more than one derivative per field. Higher order contributions to the quadratic Lagrangian for the phonon (100), can contain terms of the form:

$$\mathcal{L}_{higher-order} \supset \Lambda m^{3/2}\mu^{\frac{3}{2}-n}\partial^n\phi^n \sim \left(\Lambda m^{3/2}\mu^{3/2}\right)^{1-\frac{n}{2}}\partial^n\phi_c^n\,, \tag{122}$$

where $\partial \to \partial_t$ or $c_s\vec{\nabla}$, and $\phi_c = \Lambda^{1/2}m^{3.4}\mu^{-1/4}\phi$ is the canonical variable. The scale $\Lambda_s = \left(\Lambda m^{3/2}\mu^{3/2}\right)^{1/4}$ is the strong coupling scale, the scale suppressing higher order terms. So, higher order corrections can be neglected when:

$$\frac{1}{\Lambda_s}\frac{\partial_r^2\phi}{\partial\phi} \sim \frac{1}{\Lambda r} \ll 1\,. \tag{123}$$

Given the profile obtained in (109), which determines μ, the strong coupling scale is given by:

$$\Lambda_s \sim \text{meV}\left(\frac{M_{DM}}{10^{12}M_\odot}\right)^{3/10}\left(\frac{m}{\text{eV}}\right)^{6/5}\left(\frac{\Lambda}{\text{meV}}\right)^{2/5}\,. \tag{124}$$

Given the fiducial parameters, $\Lambda_s \sim$ meV. So, higher derivatives are suppresed if $r \gg 0.2$mm, which is clearly satisfied on astrophysical scales.

Criteria for condensate coherence

An important criteria to verify the validity of the superfluid description we are using is to check if our superfluid obeys the Landau criteria. As we saw in Section 3.2 the criteria for the system transports charge without dissipation leading to the coherence of the BEC is maintained is that the velocity of the superfluid is smaller than the critical velocity:

$$v_s \ll v_c \sim \left(\frac{\rho}{m^4}\right)^{1/3}\,. \tag{125}$$

Added with that the condition that the critical velocity cannot be non-vanishing and that the fluid needs to be in a condensate state, these criteria are the conditions for supeffluidity. In our case, in Section 4.2.1, we already evaluated the conditions for DM to be condensed in the center of galaxies.

We can estimate v_c by using the halo mass density $\rho = (2m)^{3/2}m\Lambda\sqrt{|X|} \sim 2m^2\Lambda\sqrt{\kappa}$, where we assumed MOND regime in the last equility and $\kappa = m\hat{\mu}$, which gives us:

$$v_c \sim 0.025\left(\frac{M_b}{10^{111}M_\odot}\right)^{1/6}\left(\frac{m}{\text{eV}}\right)^{-2/3}\left(\frac{\Lambda}{\text{meV}}\right)^{2/9}\left(\frac{\text{kpc}}{r}\right)^{1/3}\,. \tag{126}$$

The superfluid velocity id given by $v_s = \partial_r\phi/m \sim \sqrt{\kappa}/m$, which yields:

$$v_s \sim \left(\frac{M_b}{10^{111}M_\odot}\right)^{1/2}\left(\frac{m}{\text{eV}}\right)^{-1}\left(\frac{\Lambda}{\text{meV}}\right)^{-1/3}\left(\frac{\text{kpc}}{r}\right)\,. \tag{127}$$

With that we have that (125):

$$r \gg \left(\frac{M_b}{10^{111}M_\odot}\right)^{1/2}\left(\frac{m}{\text{eV}}\right)^{-1/2}\left(\frac{\Lambda}{\text{meV}}\right)^{-5/6}\text{kpc}\,. \tag{128}$$

We can see that this condition is satisfied in the central regions of galaxies, and we have coherence of the condensate and superfluidity in those scales.

4.2.6. Solar system

At solar system scales the bounds on deviation from standard Newtonian gravity are very tight, and these measurements do not allow deviations from the Newtonian dynamics. Full MOND is in tension with this bounds. However, the DM superfluid scenario fits well into the Solar system bounds. We can see that using the coherence bound for the condensate (125). For that we need to evaluate v_s and v_c.

The superfluid velocity in the vicinity of the Sun ($M_b = M\odot$) is given by:

$$v_s^{\odot} = 5\left(\frac{m}{\mathrm{eV}}\right)^{-1}\left(\frac{\Lambda}{\mathrm{meV}}\right)^{-1/3}\frac{\mathrm{AU}}{r}\,. \tag{129}$$

where AU is the astronomical unit, the average distance between the Earth and the Sun, and r represents the distance to the Sun. The critical velocity of the Milky Way galaxy ($M_b = 3\times 10^{11} M_{\odot}$) evaluated at our solar system ($r \sim 8$kpc) is:

$$v_c^{MW} \sim 0.02\left(\frac{m}{\mathrm{eV}}\right)^{-2/3}\left(\frac{\Lambda}{\mathrm{meV}}\right)^{-2/9}\,. \tag{130}$$

We can see that the coherence bound $v_s^{\odot} \ll v_c^{MW}$ is obeyed for distance at distances much larger than the solar system scales:

$$r \gg 250\left(\frac{m}{\mathrm{eV}}\right)^{-1/3}\left(\frac{\Lambda}{\mathrm{meV}}\right)^{-5/9}\mathrm{AU}\,. \tag{131}$$

This means that the BEC loses its coherence on distances like the solar system and DM at these scales is in the normal phase, and obeys standard Newtonian gravity.

4.2.7. Relativistic Completion

As we saw in Section 3, the description of a superfluid is given by a weakly self-interacting field theory with global U(1) symmetry. The symmetry is spontaneously broken by the superfluid ground state of a system at chemical potential μ. In the previous section, where we defined this field theory for superfluids, we added a 2-body self-interaction, $\lambda|\Psi|^4$. This gives an equation of state $P \propto n^2$. Then, given the virial expansion, $P = k_B T\rho + g_2(T)n^2 + g_2(T)n^3 + \cdots$, this suggests that to have a theory with $P \propto n^3$ we need a theory where 3-body processes are important, $\lambda|\Psi|^6$. This is indeed true.

3-body interaction:. Lets consider now like before that the self interacting theory with U(1) symmetry that gives us the superfluid has a 3-body interaction, instead of a 2-body one. The relativistic action of this theory is given by:

$$\mathcal{L} = -|\partial\Psi|^2 - m^2|\Psi|^2 - \frac{\lambda}{3}|\Psi|^6\,, \tag{132}$$

where $\lambda > 0$ for stability. Like before, this theory conserves particle number. Since we are interested in the non-relativistic (NR) theory, replacing $\Psi = \psi e^{imt}$ and taking the NR limit gives us:

$$\mathcal{L} = \frac{i}{2}\left(\psi\partial_t\psi^* - \psi^*\partial_t\psi\right) - \frac{|\vec{\nabla}\psi|^2}{2m} - \frac{\lambda}{24m^3}|\psi|^6\,. \tag{133}$$

With that, we can calculate the equation of motion, which gives us the Schrödinger's equation:

$$-i\partial_t\psi + \frac{\vec{\nabla}^2\psi}{m} - \frac{\lambda}{8m^3}|\psi|^4\psi = 0\,. \tag{134}$$

The background solution which describes the BEC at zero temperature is given by: $\psi_0 = \sqrt{2m}\,v e^{i\mu t}$, where $\mu = \lambda v^4/2m$. The excitations are given by:

$$\psi = \sqrt{2m}\,(v+\rho)e^{i}(\mu t + \phi)\,, \tag{135}$$

where ϕ is the Goldstone boson associated with the broken U(1), and ρ is the massive mode. Substituting this back into (133), and integrate out ρ, to leading order in the derivative expansion, the action is given by:

$$\mathcal{L} = \frac{4}{3}m\left(\mu + \dot{\phi} - \frac{(\vec{\nabla}\phi)^2}{2m}\right)\left[\frac{2m}{\lambda}\left(\mu + \dot{\phi} - \frac{(\vec{\nabla}\phi)^2}{2m}\right)\right]^{1/2} = \frac{4}{3}\left(\frac{2}{\lambda}\right)^{1/2} m^{3/2}\, X\sqrt{X}\,, \tag{136}$$

with $X = \mu + \dot{\phi} - (\vec{\nabla}\phi)^2/2m$. This is very promising since the theory with a 3-body interaction gives a low-energy Lagrangian with the same exponent as the one we need for MOND. However, it has the opposite sign, given that $\lambda > 0$! In this limit, the gradient term will never dominate over μ and MOND regime does not happen. As we saw before, the limit where $\lambda < 0$ is unstable.

So, the expected description as a theory with 3-body processes is does not work for the DM superfluid model, where we want to recover MOND behavior in galaxies. It was phenomenologically proposed in [121] a relativistic Lagrangian that is able to reproduce our expected Lagrangian (98)in the non-relativistic regime, and it is given by:

$$\mathcal{L} = -\frac{1}{2}\left(|\partial_\mu\Psi| + m^2|\Psi|^2\right) - \frac{\Lambda^4}{6\left(\Lambda_c^2 + |\Psi|^2\right)^6}\left(|\partial_\mu\Psi| + m^2|\Psi|^2\right)^3\,. \tag{137}$$

The scale Λ_c was introduced in order for the theory to admit $\Psi = 0$ vacuum. It is easy to see that this action reduces, in the non-relativistic limit and when $\Lambda_c \ll |\Psi|^2$, this action gives (98). The condition for MOND, given by Λ_c can be rewritten as $|X| \gtrsim \Lambda_c^4/(2m\Lambda^2)$, which corresponds to:

$$a_\phi \gtrsim \frac{\Lambda_c}{\alpha^2\Lambda}a_0\,, \tag{138}$$

where a_ϕ is the acceleration from the phonon that can be obtained from the action and given by $a_\phi = \alpha(\Lambda/M_{pl})\phi'$. According to observations, the deep MOND regime is very accurate for $\sim a_0/10$, which poses a bound for Λ_c.

4.2.8. Cosmology

After working out the galactic behavior of the DM superfluid model, we need to work out its cosmological behavior. One compelling feature of this model is that at the same time it describes the small scale behavior, it also recovers the large scale successes of CDM. In this section we show how DM superfluid behaves cosmologically.

The first question we would like to answer is if DM is in the superfluid or normal phase cosmologically. We saw in Section 4.2.1 that the critical temperature of the DM superfluid is given by (92), and T/T_c today is around 10^{-2} for massive galaxies ($M \sim 10^{12}M_\odot$). Cosmologically, the temperature in units of T_c is much colder. We can estimate that by known that light candidates for DM like ours have to be produced out-of-equilibrium like a phase transition. These non-thermal relics can be generated, for example, through a vacuum displacement mechanism[13], like the axion. So, the particles are created when $H_i \sim m$, which corresponds to a temperature for the photon-baryon plasma:

$$T_i^b \sim \sqrt{mM_{pl}} \xrightarrow[m\sim\mathrm{eV}]{} 50\mathrm{TeV}\,, \tag{139}$$

which is around the weak scale!

[13]The vacuum displacement mechanism [161] can be described, in a concise way in the following way. A massive scalar field in an FRW universe, when $H > m_\varphi$, is overdamped and it behaves nearly constant. So, if we consider that initially this field was displaced from its minimum, $\varphi = \varphi^*$, the field has a potential energy given by $varphi^*$. When $H \sim m_\varphi$, the field starts to evolve and begins to oscillate in its potential., and in turn redshifts like matter.

With that, we can rewrite the condition for thermalization (87), given that the velocity and density redshifts as $v \propto a^{-1}$ and $\rho \propto a^{-3}$. At matter-radiation equality, we can write this condition as:

$$m \sim \rho_{eq}^{1/4} \ll \left(\frac{\rho_{eq}}{v_{eq}^3}\right)^{1/4} , \tag{140}$$

where $\rho_{eq} \sim 0.4\text{eV}^4$ and by using that $v_{eq} = v_i a_i/a_{eq} \sim \text{eV}/\sqrt{mM_{pl}}$ is much smaller than one, while $v_i \sim 1$ since it was created deep into the radiation era. Since $T/T_c = (v/v_c)^2$, we have that:

$$\left(\frac{T}{T_c}\right)_{cosmo} \sim v_{eq}\left(\frac{m}{\text{eV}}\right)^{8/3} \sim 10^{-28}\left(\frac{m}{\text{eV}}\right)^{5/3} . \tag{141}$$

So, cosmologically, all the DM is in the superfluid state.

As we saw, the cosmological temperatures are many orders of magnitude different than the temperatures on galaxies. For the EFT built for the superfluid to be valid on such a scales (of time, temperature), the parameters of the EFT Λ and α need to depend evolve with temperature. This dependence is estimated in [121] by making some phenomenological statements in for the theory to match both regimes.

5. Afterword

In these notes I showed different models that describe DM as a light scalar field. They use the physics of BEC and superfluidity in order to describe the behavior of DM on galactic scales. Although these models started to appear 30 years ago, only recently they received more attention. So, these models are still very new and still need a lot of work. This work is mainly in the numerical simulation of those models on galactic and cosmological scales. For the fuzzy DM model, this endeavour is already on the way and those simulations have been revealing important features of those models. The superfluid DM model still lacks a numerical treatment. The study of how to describe the superfluid DM in a way that it can be simulated is an important future step. Another important step is to test these models consistently against the cosmological and astrophysical observations, in order to constraint the parameters of these models and test their validity. This is on the way for all the models, but it is a very important step for their validation.

Finally there is still a lot of room for theoretical development. Using analogue systems from condensed matter opened up a new class of rich phenomena that can be explored. For the models presented, important steps would be to describe the finite field theory, describe the superfluid as a two fluid system, find the UV completion of the theories, among other challenges.

In summary, the study of the class of ultra-light DM is an active area of study with many challenges still opened to be addressed theoretically, numerically and observationally.

References

[1] J. S. Bullock and M. Boylan-Kolchin, Ann. Rev. Astron. Astrophys. **55**, 343 (2017) doi:10.1146/annurev-astro-091916-055313 [arXiv:1707.04256 [astro-ph.CO]].

[2] A. Del Popolo and M. Le Delliou, Galaxies **5**, no. 1, 17 (2017) doi:10.3390/galaxies5010017 [arXiv:1606.07790 [astro-ph.CO]].

[3] B. Famaey and S. McGaugh, Living Rev. Rel. **15**, 10 (2012) doi:10.12942/lrr-2012-10 [arXiv:1112.3960 [astro-ph.CO]].

[4] F. Zwicky, Helv. Phys. Acta **6**, 110 (1933) [Gen. Rel. Grav. **41**, 207 (2009)]. doi:10.1007/s10714-008-0707-4

[5] G. Bertone and D. Hooper, Rev. Mod. Phys. **90**, no. 4, 045002 (2018) doi:10.1103/RevModPhys.90.045002 [arXiv:1605.04909 [astro-ph.CO]].

[6] V. C. Rubin and W. K. Ford, Jr., Astrophys. J. **159**, 379 (1970). doi:10.1086/150317

[7] L. Anderson *et al.* [BOSS Collaboration], Mon. Not. Roy. Astron. Soc. **441**, no. 1, 24 (2014) doi:10.1093/mnras/stu523 [arXiv:1312.4877 [astro-ph.CO]].

[8] P. A. R. Ade *et al.* [Planck Collaboration], Astron. Astrophys. **594**, A13 (2016) doi:10.1051/0004-6361/201525830 [arXiv:1502.01589 [astro-ph.CO]].

[9] M. Tegmark, M. R. Blanton, M. A. Strauss, F. Hoyle, D. Schlegel, R. Scoccimarro, M. S. Vogeley, D. H. Weinberg, I. Zehavi, A. Berlind, et al., The Astrophysical Journal 606, 702 (2004), astro-ph/0310725 .

[10] L. Roszkowski, E. M. Sessolo and S. Trojanowski, Rept. Prog. Phys. **81**, no. 6, 066201 (2018) doi:10.1088/1361-6633/aab913 [arXiv:1707.06277 [hep-ph]].

[11] P. Colin, V. Avila-Reese and O. Valenzuela, Astrophys. J. **542**, 622 (2000) doi:10.1086/317057 [astro-ph/0004115].

[12] T. Lin, arXiv:1904.07915 [hep-ph].

[13] D. N. Spergel and P. J. Steinhardt, Phys. Rev. Lett. **84**, 3760 (2000) doi:10.1103/PhysRevLett.84.3760 [astro-ph/9909386].

[14] Schneider, P.. Extragalactic Astronomy and Cosmology: An Introduction - 2015. Springer Verlag Berlin.

[15] G. L. Bryan and M. L. Norman, Astrophys. J. **495**, 80 (1998) doi:10.1086/305262 [astro-ph/9710107].

[16] J. F. Navarro, C. S. Frenk and S. D. M. White, Astrophys. J. **490**, 493 (1997) doi:10.1086/304888 [astro-ph/9611107].

[17] J. Einasto, Trudy Astrofizicheskogo Instituta Alma-Ata **5**, 87 (1965).

[18] J. F. Navarro *et al.*, Mon. Not. Roy. Astron. Soc. **349**, 1039 (2004) doi:10.1111/j.1365-2966.2004.07586.x [astro-ph/0311231].

[19] L. Gao, J. F. Navarro, S. Cole, C. Frenk, S. D. M. White, V. Springel, A. Jenkins and A. F. Neto, Mon. Not. Roy. Astron. Soc. **387**, 536 (2008) doi:10.1111/j.1365-2966.2008.13277.x [arXiv:0711.0746 [astro-ph]].

[20] B. Moore, Nature **370**, 629 (1994). doi:10.1038/370629a0

[21] R. A. Flores and J. R. Primack, Astrophys. J. **427**, L1 (1994) doi:10.1086/187350 [astro-ph/9402004].

[22] S. S. McGaugh and W. J. G. de Blok, Astrophys. J. 499, 41 (1998), astro-ph/9801123.

[23] S. Côte, C. Carignan, and K. C. Freeman, Astron. J. 120, 3027 (2000).

[24] F. C. van den Bosch and R. A. Swaters, Mon. Not. Roy. Astron. Soc. 325, 1017 (2001), astro-ph/0006048.

[25] A. Borriello and P. Salucci, Mon. Not. Roy. Astron. Soc. 323, 285 (2001), astro-ph/0001082.

[26] W. J. G. de Blok, S. S. McGaugh, and V. C. Rubin, Astron. J. 122, 2396 (2001).

[27] W. J. G. de Blok, S. S. McGaugh, A. Bosma, and V. C. Rubin, Astrophys. J. 552, L23 (2001), astro-ph/0103102.

[28] D. Marchesini, E. D'Onghia, G. Chincarini, C. Firmani, P. Conconi, E. Molinari, and A. Zacchei, Astrophys. J. 575, 801 (2002), astro-ph/0202075.

[29] Simon JD, Bolatto AD, Leroy A, Blitz L, Gates EL. 2005. ApJ 621:757–776.

[30] G. Gentile, A. Burkert, P. Salucci, U. Klein, and F. Walter, Submitted to: Astrophys. J. Lett. (2005), astro-ph/0506538.

[31] G. Gentile, P. Salucci, U. Klein, and G. L. Granato, Mon. Not. Roy. Astron. Soc. 375, 199 (2007), astro-ph/0611355.

[32] R. Kuzio de Naray, S. S. McGaugh, W. J. G. de Blok, and A. Bosma, Astrophys. J. Suppl. 165, 461 (2006), astro-ph/0604576.

[33] R.KuziodeNaray,S.S.McGaugh,andW.J.G.deBlok,Astrophys.J.676,920(2008),0712.0860.

[34] S.-H. Oh, W. J. G. de Blok, E. Brinks, F. Walter, and R. C. Kennicutt, Jr, Astron. J. 141, 193 (2011), 1011.0899.

[35] S. H. Oh *et al.*, Astron. J. **149**, 180 (2015) doi:10.1088/0004-6256/149/6/180 [arXiv:1502.01281 [astro-ph.GA]].

[36] Oman, K.A.; Navarro, J.F.; Fattahi, A.; Frenk, C.S.; Sawala, T.; White, S.D.M.; Bower, R.; Crain, R.A.; Furlong, M.; Schaller, M.; et al. The unexpected diversity of dwarf galaxy rotation curves. Mon. Not. Roy. Astro. Soc. 2015, 452, 3650–3665.

[37] Governato F, Zolotov A, Pontzen A, Christensen C, Oh SH, et al. 2012. MNRAS 422:1231–1240.

[38] Munshi F, Governato F, Brooks AM, Christensen C, Shen S, et al. 2013. ApJ 766:56.

[39] Madau P, Shen S, Governato F. 2014. ApJ 789:L17

[40] J. Oñorbe, M. Boylan-Kolchin, J. S. Bullock, P. F. Hopkins, D. Kerěs, C. A. Faucher-Giguère, E. Quataert and N. Murray, Mon. Not. Roy. Astron. Soc. **454**, no. 2, 2092 (2015) doi:10.1093/mnras/stv2072 [arXiv:1502.02036 [astro-ph.GA]].

[41] Tollet E, Maccio AV, Dutton AA, Stinson GS, Wang L, et al. 2016. MNRAS 456:3542–3552.

[42] A. Fitts *et al.*, Mon. Not. Roy. Astron. Soc. **471**, no. 3, 3547 (2017) doi:10.1093/mnras/stx1757

[43] A. Drlica-Wagner *et al.* [DES Collaboration], Astrophys. J. **813**, no. 2, 109 (2015) doi:10.1088/0004-637X/813/2/109 [arXiv:1508.03622 [astro-ph.GA]].

[44] Efstathiou G. 1992. MNRAS 256:43P–47P.

[45] Bullock JS, Kravtsov AV, Weinberg DH. 2000. ApJ 539:517–521.

[46] Benson AJ, Lacey CG, Baugh CM, Cole S, Frenk CS. 2002. MNRAS 333:156–176.

[47] Bovill MS, Ricotti M. 2009. ApJ 693:1859–1870.

[48] Sawala T, Frenk CS, Fattahi A, Navarro JF, Bower RG, et al. 2016. MNRAS 457:1931–1943.

[49] A. Dekel and J. Silk, Astrophys. J. 303, 39 (1986).

[50] Zolotov, A.; Brooks, A.M.; Willman, B.; Governato, F.; Pontzen, A.; Christensen, C.; Dekel, A.; Quinn, T.; Shen, S.; Wadsley, J., Astrophys. J. 2012, 761, 71.

[51] Sawala, T.; Fren, C.S.; Fattahi, A.; Navarro, J.F.; Bower, R.G.; Crain, R.A.; Vecchia, C.D.; Furlong, M.; Helly, J.C.; Jenkins, A.; et al, Mon. Not. R. Astron. Soc. 2016, 457, 1931–1943.

[52] Zhu, Q.; Marinacci, F.; Maji, M.; Li, Y.; Springel, V.; Hernquist, L, Mon. Not. Roy. Astro. Soc. 2016, 458, 1559–1580.

[53] Boylan-Kolchin M, Bullock JS, Kaplinghat M, MNRAS 415:L40–L44, 2011.

[54] Boylan-Kolchin M, Bullock JS, Kaplinghat M, MNRAS 422:1203–1218, 2012

[55] Ferrero, I.; Abadi, M.G.; Navarro, J.F.; Sales, L.V.; Gurovich, S, Mon. Not. Roy. Astro. Soc. 2012, 425, 2817–2823.

[56] Papastergis, E.; Giovanelli, R.; Haynes, M.P.; Shankar, F., Astron. Astrophys. 2015, 574, A113.

[57] Garrison-Kimmel, S.; Boylan-Kolchin, M.; Bullock, J.S.; Kirby, E.N, Mon. Not. Roy. Astro. Soc. 2014, 444, 222–236.

[58] Jeremiah P. Ostriker, Ena Choi, Anthony Chow, Kundan Guha, [arXiv:1904.10471[astro-ph]].

[59] M. Milgrom, "A Modification of the Newtonian dynamics as a possible alternative to the hidden mass hypothesis," Astrophys. J. 270, 365.

[60] McGaugh:2007fj S. S. McGaugh, Astrophys. J. **632**, 859 (2005) doi:10.1086/432968 [astro-ph/0506750].

[61] S. S. McGaugh, IAU Symp. **244**, 136 (2008) doi:10.1017/S1743921307013920 [arXiv:0707.3795 [astro-ph]].

[62] S. McGaugh, F. Lelli and J. Schombert, Phys. Rev. Lett. **117**, no. 20, 201101 (2016) doi:10.1103/PhysRevLett.117.201101 [arXiv:1609.05917 [astro-ph.GA]]. (1983).

[63] F. Lelli, S. S. McGaugh, J. M. Schombert and M. S. Pawlowski, Astrophys. J. **836**, no. 2, 152 (2017) doi:10.3847/1538-4357/836/2/152 [arXiv:1610.08981 [astro-ph.GA]].

[64] F. Lelli, S. S. McGaugh and J. M. Schombert, Astrophys. J. **816**, no. 1, L14 (2016) doi:10.3847/2041-8205/816/1/L14 [arXiv:1512.04543 [astro-ph.GA]].

[65] F. Lelli, S. S. McGaugh, J. M. Schombert and M. S. Pawlowski, Astrophys. J. **827**, no. 1, L19 (2016) doi:10.3847/2041-8205/827/1/L19 [arXiv:1607.02145 [astro-ph.GA]].

[66] H. Desmond, Mon. Not. Roy. Astron. Soc. **464**, no. 4, 4160 (2017) doi:10.1093/mnras/stw2571 [arXiv:1607.01800 [astro-ph.GA]].

[67] M. Milgrom, "A Modification of the Newtonian dynamics: Implications for galaxies," Astro- phys. J. 270, 371 (1983).

[68] M. Milgrom, "A modification of the Newtonian dynamics: implications for galaxy systems," Astrophys. J. 270, 384 (1983).

[69] R. H. Sanders and S. S. McGaugh, Ann. Rev. Astron. Astrophys. **40**, 263 (2002) doi:10.1146/annurev.astro.40.060401.093923 [astro-ph/0204521].

[70] A. H. Broeils, "Dark and visible matter in spiral galaxies," PhD Dissertation, Univ. of Gronin- gen, The Netherlands (1992).

[71] K. G. Begeman, A. H. Broeils and R. H. Sanders, Mon. Not. Roy. Astron. Soc. **249**, 523 (1991).

[72] J. Bekenstein and M. Milgrom, Astrophys. J. **286**, 7 (1984). doi:10.1086/162570

[73] J. F. Navarro, A. Benítez-Llambay, A. Fattahi, C. S. Frenk, A. D. Ludlow, K. A. Oman, M. Schaller and T. Theuns, Mon. Not. Roy. Astron. Soc. **471**, no. 2, 1841 (2017) doi:10.1093/mnras/stx1705 [arXiv:1612.06329 [astro-ph.GA]].

[74] I. Ferrero, J. F. Navarro, M. G. Abadi, L. V. Sales, R. G. Bower, R. A. Crain, C. S. Frenk, M. Schaller, J. Schaye, T. Theuns, Mon. Not. Roy. Astron. Soc. **464**, no. 4, 4736 (2017), doi.org/10.1093/mnras/stw2691 [arXiv:1607.03100 [astro-ph.GA]].

[75] E. Garaldi, E. Romano-Díaz, C. Porciani and M. S. Pawlowski, Phys. Rev. Lett. **120**, no. 26, 261301 (2018) doi:10.1103/PhysRevLett.120.261301 [arXiv:1712.04448 [astro-ph.GA]].

[76] A. A. Dutton, A. V. Macciò, A. Obreja and T. Buck, doi:10.1093/mnras/stz531 arXiv:1902.06751 [astro-ph.GA].

[77] J. F. Navarro, arXiv:1811.02025 [astro-ph.GA].

[78] M. Borzyszkowski, C. Porciani, E. Romano-Diaz and E. Garaldi, Mon. Not. Roy. Astron. Soc. **469**, no. 1, 594 (2017) doi:10.1093/mnras/stx873 [arXiv:1610.04231 [astro-ph.CO]].

[79] E. Romano-Diaz, E. Garaldi, M. Borzyszkowski and C. Porciani, Mon. Not. Roy. Astron. Soc. **469**, no. 2, 1809 (2017) doi:10.1093/mnras/stx878 [arXiv:1701.02743 [astro-ph.GA]].

[80] E. Garaldi, E. Romano-Díaz, M. Borzyszkowski and C. Porciani, Mon. Not. Roy. Astron. Soc. **473**, no. 2, 2234 (2017) doi:10.1093/mnras/stx2489 [arXiv:1707.01108 [astro-ph.GA]].

[81] L. Wang, A. A. Dutton, G. S. Stinson, A. V. Macciò, C. Penzo, X. Kang, B. W. Keller and J. Wadsley, Mon. Not. Roy. Astron. Soc. **454**, no. 1, 83 (2015) doi:10.1093/mnras/stv1937 [arXiv:1503.04818 [astro-ph.GA]].

[82] http://www.illustris-project.org/

[83] J. Schaye *et al.*, Mon. Not. Roy. Astron. Soc. **446**, 521 (2015) doi:10.1093/mnras/stu2058 [arXiv:1407.7040 [astro-ph.GA]].

[84] R. A. Crain *et al.*, Mon. Not. Roy. Astron. Soc. **450**, no. 2, 1937 (2015) doi:10.1093/mnras/stv725 [arXiv:1501.01311 [astro-ph.GA]].

[85] T. Sawala *et al.*, Mon. Not. Roy. Astron. Soc. **457**, no. 2, 1931 (2016) doi:10.1093/mnras/stw145 [arXiv:1511.01098 [astro-ph.GA]].

[86] P. Kapitza, Nature **141**, 74 (1938) doi.org/10.1038/141074a0.

[87] J. F. Allen & A. D. Misener, Nature **142**, 643 (1938) doi.org/10.1038/142643a0.

[88] L. D. Landau and E. M. Lifshitz, "Textbook On Theoretical Physics. Vol. 5: Statistical Physics Part I," Butterworth-Heinemann, Oxford UK (1997) 544p.

[89] Pitaevskii, Lev, and Sandro Stringari. "Superfluidity." In Bose-Einstein Condensation and Superfluidity. Oxford: Oxford University Press, 2016.

[90] M. Greiter, F. Wilczek and E. Witten, Mod. Phys. Lett. B **3**, 903 (1989). doi:10.1142/S0217984989001400

[91] D. T. Son and M. Wingate, Annals Phys. **321**, 197 (2006) doi:10.1016/j.aop.2005.11.001 [cond-mat/0509786].

[92] S. J. Sin, Phys. Rev. D **50**, 3650 (1994) doi:10.1103/PhysRevD.50.3650 [hep-ph/9205208].

[93] S. U. Ji and S. J. Sin, Phys. Rev. D **50**, 3655 (1994) doi:10.1103/PhysRevD.50.3655 [hep-ph/9409267].

[94] A. Sharma, J. Khoury and T. Lubensky, arXiv:1809.08286 [hep-th].

[95] J. W. Lee, EPJ Web Conf. **168**, 06005 (2018) doi:10.1051/epjconf/201816806005 [arXiv:1704.05057 [astro-ph.CO]].

[96] J. Goodman, New Astron. **5**, 103 (2000) doi:10.1016/S1384-1076(00)00015-4 [astro-ph/0003018].

[97] P. J. E. Peebles, Astrophys. J. **534**, L127 (2000) doi:10.1086/312677 [astro-ph/0002495].

[98] M. P. Silverman and R. L. Mallett, Gen. Rel. Grav. **34**, 633 (2002). doi:10.1023/A:1015934027224

[99] A. Arbey, J. Lesgourgues and P. Salati, Phys. Rev. D **68**, 023511 (2003) doi:10.1103/PhysRevD.68.023511 [astro-ph/0301533].

[100] C. G. Boehmer and T. Harko, JCAP **0706**, 025 (2007) doi:10.1088/1475-7516/2007/06/025 [arXiv:0705.4158 [astro-ph]].

[101] J. W. Lee, Phys. Lett. B **681**, 118 (2009) doi:10.1016/j.physletb.2009.10.005 [arXiv:0805.2877 [astro-ph]].

[102] J. W. Lee and S. Lim, JCAP **1001**, 007 (2010) doi:10.1088/1475-7516/2010/01/007 [arXiv:0812.1342 [astro-ph]].

[103] T. Harko, JCAP **1105**, 022 (2011) doi:10.1088/1475-7516/2011/05/022 [arXiv:1105.2996 [astro-ph.CO]].

[104] T. Rindler-Daller and P. R. Shapiro, Mon. Not. Roy. Astron. Soc. **422**, 135 (2012) doi:10.1111/j.1365-2966.2012.20588.x [arXiv:1106.1256 [astro-ph.CO]].

[105] Z. Slepian and J. Goodman, Mon. Not. Roy. Astron. Soc. **427**, 839 (2012) doi:10.1111/j.1365-2966.2012.21901.x [arXiv:1109.3844 [astro-ph.CO]].

[106] M. Dwornik, Z. Keresztes and L. Á. Gergely, arXiv:1312.3715 [gr-qc].

[107] F. S. Guzmán, F. D. Lora-Clavijo, J. J. González-Avilés and F. J. Rivera-Paleo, Phys. Rev. D **89**, no. 6, 063507 (2014) doi:10.1103/PhysRevD.89.063507 [arXiv:1310.3909 [astro-ph.CO]].

[108] T. Harko, Phys. Rev. D **89**, no. 8, 084040 (2014) doi:10.1103/PhysRevD.89.084040 [arXiv:1403.3358 [gr-qc]].

[109] J. Fan, Phys. Dark Univ. **14**, 84 (2016) doi:10.1016/j.dark.2016.10.005 [arXiv:1603.06580 [hep-ph]].

[110] E. Seidel and W. M. Suen, Phys. Rev. D **42**, 384 (1990). doi:10.1103/PhysRevD.42.384

[111] L. M. Widrow and N. Kaiser, Astrophys. J. **416**, L71 (1993).

[112] J. H. H. Chan , Hsi-Yu Schive, Tak-Pong Woo and Tzihong Chiueh Mon. Not. Roy. Astron. Soc. **478**, no. 2, 2686 (2018) doi.org/10.1093/mnras/sty900 [arXiv:1712.01947 [astro-ph.GA]].

[113] W. Hu, R. Barkana and A. Gruzinov, Phys. Rev. Lett. **85**, 1158 (2000) doi:10.1103/PhysRevLett.85.1158 [astro-ph/0003365].

[114] L. Hui, J. P. Ostriker, S. Tremaine and E. Witten, Phys. Rev. D **95**, no. 4, 043541 (2017) doi:10.1103/PhysRevD.95.043541 [arXiv:1610.08297 [astro-ph.CO]].

[115] O. Erken, P. Sikivie, H. Tam and Q. Yang, Phys. Rev. D **85**, 063520 (2012) doi:10.1103/PhysRevD.85.063520 [arXiv:1111.1157 [astro-ph.CO]].

[116] P. Sikivie and Q. Yang, Phys. Rev. Lett. **103**, 111301 (2009) doi:10.1103/PhysRevLett.103.111301 [arXiv:0901.1106 [hep-ph]].

[117] D. J. E. Marsh, Phys. Rept. **643**, 1 (2016) doi:10.1016/j.physrep.2016.06.005 [arXiv:1510.07633 [astro-ph.CO]].

[118] A. H. Guth, M. P. Hertzberg and C. Prescod-Weinstein, Phys. Rev. D **92**, no. 10, 103513 (2015) doi:10.1103/PhysRevD.92.103513 [arXiv:1412.5930 [astro-ph.CO]].

[119] A. Suárez, V. H. Robles and T. Matos, Astrophys. Space Sci. Proc. **38**, 107 (2014) doi:10.1007/978-3-319-02063-1_9 [arXiv:1302.0903 [astro-ph.CO]].

[120] L. Berezhiani and J. Khoury, Phys. Lett. B **753**, 639 (2016) doi:10.1016/j.physletb.2015.12.054 [arXiv:1506.07877 [astro-ph.CO]].

[121] L. Berezhiani and J. Khoury, Phys. Rev. D **92**, 103510 (2015) doi:10.1103/PhysRevD.92.103510 [arXiv:1507.01019 [astro-ph.CO]].

[122] J. Khoury, Phys. Rev. D **93**, no. 10, 103533 (2016) doi:10.1103/PhysRevD.93.103533 [arXiv:1602.05961 [astro-ph.CO]].

[123] A. Hodson, H. Zhao, J. Khoury and B. Famaey, Astron. Astrophys. **607**, A108 (2017) doi:10.1051/0004-6361/201630069 [arXiv:1611.05876 [astro-ph.CO]].

[124] L. Berezhiani, B. Famaey and J. Khoury, JCAP **1809**, no. 09, 021 (2018) doi:10.1088/1475-7516/2018/09/021 [arXiv:1711.05748 [astro-ph.CO]].

[125] R. Hlozek, D. Grin, D. J. E. Marsh and P. G. Ferreira, Phys. Rev. D **91**, no. 10, 103512 (2015) doi:10.1103/PhysRevD.91.103512 [arXiv:1410.2896 [astro-ph.CO]].

[126] H. Y. Schive, T. Chiueh, T. Broadhurst and K. W. Huang, Astrophys. J. **818**, no. 1, 89 (2016) doi:10.3847/0004-637X/818/1/89 [arXiv:1508.04621 [astro-ph.GA]].

[127] P. S. Corasaniti, S. Agarwal, D. J. E. Marsh and S. Das, Phys. Rev. D **95**, no. 8, 083512 (2017) doi:10.1103/PhysRevD.95.083512 [arXiv:1611.05892 [astro-ph.CO]].

[128] A. W. McConnachie, Astron. J. **144**, 4 (2012) doi:10.1088/0004-6256/144/1/4 [arXiv:1204.1562 [astro-ph.CO]].

[129] S. R. Chen, H. Y. Schive and T. Chiueh, Mon. Not. Roy. Astron. Soc. **468**, no. 2, 1338 (2017) doi:10.1093/mnras/stx449 [arXiv:1606.09030 [astro-ph.GA]].

[130] H. Y. Schive, T. Chiueh and T. Broadhurst, Nature Phys. **10**, 496 (2014) doi:10.1038/nphys2996 [arXiv:1406.6586 [astro-ph.GA]].

[131] B. Schwabe, J. C. Niemeyer and J. F. Engels, Phys. Rev. D **94**, no. 4, 043513 (2016) doi:10.1103/PhysRevD.94.043513 [arXiv:1606.05151 [astro-ph.CO]].

[132] H. Y. Schive, M. H. Liao, T. P. Woo, S. K. Wong, T. Chiueh, T. Broadhurst and W.-Y. P. Hwang, Phys. Rev. Lett. **113**, no. 26, 261302 (2014) doi:10.1103/PhysRevLett.113.261302 [arXiv:1407.7762 [astro-ph.GA]].

[133] J. Veltmaat and J. C. Niemeyer, Phys. Rev. D **94**, no. 12, 123523 (2016) doi:10.1103/PhysRevD.94.123523 [arXiv:1608.00802 [astro-ph.CO]].

[134] T. Kobayashi, R. Murgia, A. De Simone, V. Iršič and M. Viel, Phys. Rev. D **96**, no. 12, 123514 (2017) doi:10.1103/PhysRevD.96.123514 [arXiv:1708.00015 [astro-ph.CO]].

[135] J. Zhang, J. L. Kuo, H. Liu, Y. L. S. Tsai, K. Cheung and M. C. Chu, Astrophys. J. **863**, 73 (2018) doi:10.3847/1538-4357/aacf3f [arXiv:1708.04389 [astro-ph.CO]].

[136] J. Zhang, H. Liu and M. C. Chu, doi:10.3389/fspas.2018.00048 arXiv:1809.09848 [astro-ph.CO].

[137] S. W. Randall, M. Markevitch, D. Clowe, A. H. Gonzalez and M. Bradac, Astrophys. J. **679**, 1173 (2008) doi:10.1086/587859 [arXiv:0704.0261 [astro-ph]].

[138] R. Massey, T. Kitching and D. Nagai, Mon. Not. Roy. Astron. Soc. **413**, 1709 (2011) doi:10.1111/j.1365-2966.2011.18246.x [arXiv:1007.1924 [astro-ph.CO]].

[139] D. Harvey, R. Massey, T. Kitching, A. Taylor and E. Tittley, Science **347**, 1462 (2015) doi:10.1126/science.1261381 [arXiv:1503.07675 [astro-ph.CO]].

[140] M. P. SilvermanR. L. Mallett, General Relativity and Gravitation, **34**, no. 5, 633 (2002) doi.org/10.1023/A:1015934027224

[141] E. C. Ostriker, Astrophys. J. **513**, 252 (1999) doi:10.1086/306858 [astro-ph/9810324].

[Lane-Emden] . Chandrasekhar, "An introduction to the study of stellar structure," Dover Publications, New York (1957).

[143] A. Nicolis, arXiv:1108.2513 [hep-th].

[144] R. B. Tully, E. J. Shaya, I. D. Karachentsev, H. M. Courtois, D. D. Kocevski, L. Rizzi and A. Peel, Astrophys. J. **676**, 184 (2008) doi:10.1086/527428 [arXiv:0705.4139 [astro-ph]].

[145] E. Noordermeer, J. M. van der Hulst, R. Sancisi, R. S. Swaters and T. S. van Albada, Mon. Not. Roy. Astron. Soc. **376**, 1513 (2007) doi:10.1111/j.1365-2966.2007.11533.x [astro-ph/0701731].

[146] A. Mahdavi, H. y. Hoekstra, A. y. Babul, D. y. Balam and P. Capak, Astrophys. J. **668**, 806 (2007) doi:10.1086/521383 [arXiv:0706.3048 [astro-ph]].

[147] M. J. Jee, A. Mahdavi, H. Hoekstra, A. Babul, J. J. Dalcanton, P. Carroll and P. Capak, Astrophys. J. **747**, 96 (2012) doi:10.1088/0004-637X/747/2/96 [arXiv:1202.6368 [astro-ph.CO]].

[148] D. Clowe, M. Markevitch, M. Bradac, A. H. Gonzalez, S. M. Chung, R. Massey and D. Zaritsky, Astrophys. J. **758**, 128 (2012) doi:10.1088/0004-637X/758/2/128 [arXiv:1209.2143 [astro-ph.CO]].

[149] M. J. Jee, H. Hoekstra, A. Mahdavi and A. Babul, Astrophys. J. **783**, 78 (2014) doi:10.1088/0004-637X/783/2/78 [arXiv:1401.3356 [astro-ph.CO]].

[150] V. Springel and G. Farrar, Mon. Not. Roy. Astron. Soc. **380**, 911 (2007) doi:10.1111/j.1365-2966.2007.12159.x [astro-ph/0703232 [ASTRO-PH]].

[151] C. Lage, G. R. Farrar, JCAP, **2015**, no. 2, 38 (2015) DOI: 10.1088/1475-7516/2015/02/038 [arXiv:1406.6703 [astro-ph.GA]].

[152] D. Harvey, R. Massey, T. Kitching, A. Taylor and E. Tittley, Science **347**, 1462 (2015) doi:10.1126/science.1261381 [arXiv:1503.07675 [astro-ph.CO]].

[153] C. Hamner, J. J. Chang, P. Engels, and M. A. Hoefer, Phys.Rev.Lett.,106,065302 (2011).

[154] J. A. Gonzalez and F. S. Guzman, Phys. Rev. D **83**, 103513 (2011) doi:10.1103/PhysRevD.83.103513 [arXiv:1105.2066 [astro-ph.CO]].

[155] A. P. Cooper *et al.*, Astrophys. J. **743**, L21 (2011) doi:10.1088/2041-8205/743/1/L21 [arXiv:1111.2864 [astro-ph.GA]].

[156] S. Hossenfelder and T. Mistele, JCAP **1902**, 001 (2019) doi:10.1088/1475-7516/2019/02/001 [arXiv:1809.00840 [astro-ph.GA]].

[157] B. P. Abbott *et al.* [LIGO Scientific and Virgo Collaborations], Phys. Rev. Lett. **119**, no. 16, 161101 (2017) doi:10.1103/PhysRevLett.119.161101 [arXiv:1710.05832 [gr-qc]].

[158] S. Boran, S. Desai, E. O. Kahya and R. P. Woodard, Phys. Rev. D **97**, no. 4, 041501 (2018) doi:10.1103/PhysRevD.97.041501 [arXiv:1710.06168 [astro-ph.HE]].

[159] R. G. Cai, T. B. Liu and S. J. Wang, Phys. Rev. D **97**, no. 2, 023027 (2018) doi:10.1103/PhysRevD.97.023027 [arXiv:1710.02425 [hep-ph]].

[160] S. Alexander, E. McDonough and D. N. Spergel, JCAP **1805**, no. 05, 003 (2018) doi:10.1088/1475-7516/2018/05/003 [arXiv:1801.07255 [hep-th]].

[161] S. M. Carroll, doi:10.1142/9789812799630_0004 [hep-th/0011110].